

# Dualities and the phase diagram of the $p$ -clock model

G. Ortiz<sup>1,1</sup>, E. Cobanera<sup>1</sup>, and Z. Nussinov<sup>2</sup>

<sup>1</sup>*Department of Physics, Indiana University, Bloomington, IN 47405, USA,*

<sup>2</sup>*Department of Physics, Washington University, St. Louis, MO 63160, USA.*

---

## Abstract

A new “bond-algebraic” approach to duality transformations provides a very powerful technique to analyze elementary excitations in the classical two-dimensional XY and  $p$ -clock models. By combining duality and Peierls arguments, we establish the existence of non-Abelian symmetries, the phase structure, and transitions of these models, unveil the nature of their topological excitations, and explicitly show that a continuous U(1) symmetry emerges when  $p \geq 5$ . This latter symmetry is associated with the appearance of discrete vortices and Berezinskii-Kosterlitz-Thouless-type transitions. We derive a correlation inequality to prove that the intermediate phase, appearing for  $p \geq 5$ , is critical (massless) with decaying power-law correlations.

*Keywords:*

$p$ -clock model, XY model, BKT transition, topological excitations, discrete vortices, Peierls argument, Griffiths inequality, duality, bond algebras

---

## 1. Introduction

In this article we investigate, via the use of *dualities*, two-dimensional ( $D = 2$ ) classical systems, such as the XY and clock models [1, 2], that display Berezinskii-Kosterlitz-Thouless (BKT)-type transitions [3, 4, 5, 6]. BKT transitions, notably characterized by essential singularities in the free energy, emerge in many physical situations including screening in Coulomb gases [7], surface roughening [8], melting in  $D = 2$  solids [4, 9], and many other classical and quantum problems, such as deconfinement in  $D = 3 + 1$  lattice gauge theories [10, 11, 12, 13]. We study these models by invoking

---

<sup>1</sup>Corresponding author: ortizg@indiana.edu

a *bond-algebraic* approach that we have recently developed [12, 13, 14, 15]. Within our duality-based method, one relates singularities in the free energy at one temperature (or coupling constants) to those at a dual temperature (or dual coupling constants).

Specifically, we investigate exact dualities of the  $D = 2$  XY and  $p$ -clock models, and exploit those dualities to unravel their phase structures. Those transformations are exact even for finite systems after appropriate boundary terms are included. It is noteworthy that unlike nearly all of the analytical work done to date, our dualities do not rely on the approximation scheme of Villain [16, 10, 17, 18], yet they can be related to the exact dualities of the Villain model in appropriate limits. Furthermore, our analysis leads to exact dualities for general  $p$ -clock models and yields a better understanding of the appearance of two transitions in systems with  $p \geq 5$  states (the XY model with only one transition is recovered in the  $p \rightarrow \infty$  limit). By fusing our duality results with the *Peierls argument*, we will be able to (1) prove that  $p \geq 5$  clock systems can be made to be self-dual; (2) prove by a Peierls argument that there exists a lower ordering temperature  $T^{(1)} \sim 1/p^2$ , associated to domain-wall excitations, below which the global  $\mathbb{Z}_p$  symmetry is broken; (3) demonstrate that a second transition occurs at a temperature  $T^{(2)} \sim \mathcal{O}(1)$  when  $p \geq 5$  (in the self-dual case, it follows that if  $T^{(1)}$  is not the self-dual temperature  $T^*$ , then there must necessarily be a second phase transition at  $T^{(2)}$  of an identical character); and (4) characterize the nature of the topological excitations, and further explain that at  $p = 5$  a new type of topological excitation, with an associated discrete winding number, appears. Our considerations suggest that these *discrete vortices* may proliferate above the temperature  $T^{(2)}$ . We will also (5) determine an analytic expression for the self-dual temperature  $T^*$ , which relates and clarifies temperature scales discussed in [19], and most importantly, (6) establish the non-Abelian polyhedral symmetry group  $P(2, 2, p)$  of the  $p$ -clock and related models, and explicitly unveil the U(1) continuous symmetry that *emerges* when  $p \geq 5$ . Indeed, the latter is intimately tied to the existence of the BKT transition. Finally, (7) we derive a correlation inequality to prove that the intermediate phase, appearing for  $p \geq 5$ , is critical (massless) with decaying power-law correlations.

Despite several analytic [10, 20, 21] and numerical calculations [22, 19, 23], the precise nature of the two phase transitions ( $p \geq 5$ ) is not completely understood. It was proven [21] that for large enough  $p$ , clock models exhibit a BKT-type transition (actually, it has only been proved that there exists

an intermediate critical phase with power-law correlations). The question whether that still holds when  $p = 5$  remains open [22]. By relying on exact results, we shed light on the character of the BKT transitions in these systems. We will relate the BKT transition to a continuous U(1) emergent symmetry of an usual type. Although BKT transitions are often discussed in terms of specific anomalous exponents and jumps in the helicity modulus, we will not address such non-universal issues.

Our treatment of classical dualities is based on a new approach developed in Refs. [14, 13] that relies on the transfer matrix or operator formalism [11]. In statistical mechanics, two models  $a$  and  $b$  are dual if their partition functions  $\mathcal{Z}_a = \text{tr} [T_a^N]$  and  $\mathcal{Z}_b = \text{tr} [T_b^N]$  are related as ( $N$  is the linear size of the system in  $D = 2$ )

$$\mathcal{Z}_a[K] = A(K, K^*)\mathcal{Z}_b[K^*], \quad (1)$$

with  $A$  some analytic function of the set of couplings  $K$  of model  $a$ , and dual couplings  $K^*$ . In principle, Eq. (1) establishes an extremely broad relationship that could be achieved through many transformation schemes, including the standard one based on taking the Fourier transform of individual Boltzmann weights [17, 24]. However, it was discovered in Refs. [14, 13] that low-temperature(strong coupling)/high-temperature(weak coupling) dualities correspond to a unitary equivalence of transfer matrices or operators,  $T_a$  and  $T_b$ ,

$$T_b = \mathcal{U}_d T_a \mathcal{U}_d^\dagger, \quad (2)$$

with  $\mathcal{U}_d$  a unitary operator. This observation is extremely insightful because there is a simple and systematic way to look for unitary equivalences between physical operators, based on the notion of *bond algebra*, or algebra of interactions [14, 13].

The outline of this article is as follows. In Section 2 we define the classical XY model, and then in 2.1 *establish its transfer operator*. In Section 2.2 we discuss the form of the exact one-dimensional quantum analogue whose partition function is that of the  $D = 2$  classical XY model with coupling constants  $K_1$  and  $K_2$ . In the limit of large coupling  $K_2$  along columns, the quantum model is the O(2) quantum rotor model. In Section 2.3, we establish the duality of the  $D = 2$  XY model to a solid-on-solid-like and also to a lattice Coulomb gas-like models and, moreover, determine the disorder variables. These dualities do not rely on the Villain approximation scheme but are *exact dualities* obtained by our bond-algebraic method [13].

We next proceed to analyze in Section 3 the  $p$ -clock model [1]. This model provides a particular controlled limit to the XY model (the  $p \rightarrow \infty$  limit). We replicate the same steps undertaken in the analysis of the XY model of Section 2, but now the Weyl algebra [25] and the theory of circulant matrices [26] play a key role. We construct in Section 3.1 its transfer matrix, and proceed in 3.2 to establish the corresponding one-dimensional quantum Hamiltonian, that is not self-dual for  $p \geq 5$ . We study the dualities of these systems in Section 3.3. The system is exactly self-dual for  $p = 2, 3, 4$ , and becomes approximately self-dual for  $K_2 \gg K_1$  when  $p \geq 5$ . In Section 3.4 we introduce a variant of the classical  $p$ -clock model that is exactly self-dual for all  $p$ . We examine, in Section 3.5, the exact and emergent symmetries of these systems and, notably, unveil the  $U(1)$  symmetry that emerges when  $p \geq 5$ . This continuous emergent symmetry is responsible for the existence of the intermediate critical (massless) phase.

Finally, in Section 4 we utilize our previous findings to better understand the phase diagram of the  $p$ -clock model. Here we present an analytic expression for the self-dual temperature  $T^*$ , an important scale in the problem, and advance a Peierls argument. We also introduce a topological invariant, that we call the discrete winding number  $k$ , to unravel the nature of the topological excitations. Starting at  $p \geq 5$  a new type of topological excitation appears with a non-zero value of  $k$  that one may call discrete vortex, and which is responsible for the phase transition to a disordered state. Domain-wall topological excitations are key at low-temperatures and their energy cost depends on  $p$ , and on the relative spin configurations (except for  $2 \leq p \leq 4$ ). By using both duality and energy-versus-entropy balance considerations we show that the transition from the critical to the disordered phase scales as  $T^{(2)} \sim \mathcal{O}(1)$ , while the one from the broken  $\mathbb{Z}_p$  symmetry to the critical phase goes as  $T^{(1)} \sim 1/p^2$  for large  $p$ . We derive a correlation inequality, i.e., show that the two-point correlation function  $G$  is a monotonically decreasing function of temperature, allowing us to prove that, for  $p \geq 5$ , the intermediate phase is critical (massless) with decaying power-law correlations. The appendices provide technical developments including a duality of the XY model to  $q$ -deformed bosons, illustrating the key physical difference between compact and non-compact degrees of freedom.

## 2. The XY model: A paradigm of BKT phenomenology

The  $D = 2$  classical XY model is the paradigmatic example of a system displaying a BKT transition at a finite temperature  $T_{\text{BKT}}^{(2)} > 0$ . This model, also known as planar rotator or planar  $O(2)$ , consists of an  $N \times N$  array of classical two-component spins  $\mathbf{S}_r$  located at the vertices  $\mathbf{r} = i \mathbf{e}_1 + j \mathbf{e}_2$  ( $i, j$  being integers) of a square lattice with unit vectors  $\mathbf{e}_\mu$ ,  $\mu = 1, 2$ , as indicated in Fig. 1. Its partition function is

$$\mathcal{Z}_{\text{XY}}[K_\mu, \mathbf{h}] = \sum_{\{\mathbf{S}_r\}} \exp \left[ \sum_{\mathbf{r}} \left( \sum_{\mu=1,2} K_\mu \mathbf{S}_{r+\mathbf{e}_\mu} \cdot \mathbf{S}_r + \mathbf{h} \cdot \mathbf{S}_r \right) \right], \quad (3)$$

where the spin  $\mathbf{S}_r = S_r^x \mathbf{e}_1 + S_r^y \mathbf{e}_2$ , the coupling  $K_\mu = \beta J_\mu$  is the product of the inverse temperature  $\beta = 1/k_B T$  and the exchange coupling  $J_\mu$ , and  $\mathbf{h}$  is a temperature-rescaled external magnetic field. Fixing the magnitude of the spin variable  $\mathbf{S}_r^2$  to one allows us to re-write the partition function as

$$\mathcal{Z}_{\text{XY}}[K_\mu, h] = \sum_{\{\theta_r\}} \exp \left[ \sum_{\mathbf{r}} \left( \sum_{\mu=1,2} K_\mu \cos(\theta_{r+\mathbf{e}_\mu} - \theta_r) + h \cos \theta_r \right) \right], \quad (4)$$

where the continuous angle variables  $\theta_r$  take values in the interval  $\theta_r = \theta_{i,j} \in [0, 2\pi)$ , i.e., it is a compact variable. We assume, without loss of generality, that  $\mathbf{h} = h \mathbf{e}_1$ . The sum over configurations represents an integral

$$\sum_{\{\theta_r\}} = \int_0^{2\pi} \prod_{\mathbf{r}} d\theta_r. \quad (5)$$

In the remainder of this article, we will concentrate on the case with zero external magnetic field, i.e.,  $h = 0$ . The XY model displays a (global) continuous  $U(1)$  symmetry, which amounts to the invariance of the model under a simultaneous rotation of every spin in the lattice by the same angle. In low dimensional systems with continuous symmetries, such as the XY model above, long-range order is more fragile. Thermal fluctuations may induce instabilities with the end result that long-range order is actually non-existent in  $D \leq 2$  dimensions. Spin-wave excitations are responsible for destroying such an order. The *Mermin-Wagner theorem* formalizes this qualitative picture. In the context of the  $D = 2$  XY model, the theorem states that this system does not display spontaneous magnetization at finite temperatures.

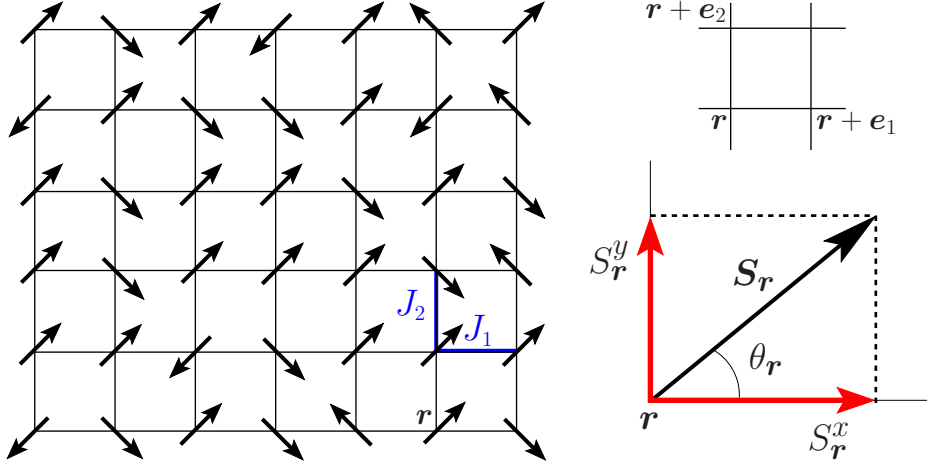


Figure 1: The two-dimensional classical XY model. On each vertex  $\mathbf{r} = i \mathbf{e}_1 + j \mathbf{e}_2$  of the square lattice there is a classical spin  $\mathbf{S}_r = S_r^x \mathbf{e}_1 + S_r^y \mathbf{e}_2$  of magnitude 1, i.e.,  $\mathbf{S}_r \cdot \mathbf{S}_r = 1$ , and  $S_r^x = \cos \theta_r$ ,  $S_r^y = \sin \theta_r$  with  $\theta_r \in [0, 2\pi)$ . Nearest neighbor spins interact with an exchange constant value  $J_1$  or  $J_2$  depending on the spatial direction.

A common physical mechanism behind the formal proofs for both classical and quantum versions of the XY model, can be found in Ref. [11].

A phase transition is said to occur whenever a thermodynamic function of the system under study displays a non-analyticity. The latter may occur even when the ground state is unique, so that there is *no* spontaneous symmetry breakdown. This is the case for the  $D = 2$  XY model, that is known to have a special phase transition at a finite, non-zero temperature  $T_{\text{BKT}}^{(2)}$ . This BKT *transition* is characterized by an essential singularity in the free energy and correlation length at  $T_{\text{BKT}}^{(2)}$ . If  $T > T_{\text{BKT}}^{(2)}$ , the correlators of the XY model decay exponentially with distance, as is typical of a disordered, paramagnetic phase. In the low-temperature phase,  $T < T_{\text{BKT}}^{(2)}$ , the correlators decay algebraically with distance, just as if every temperature below  $T_{\text{BKT}}^{(2)}$  represented an ordinary critical point. The fact that this power-law behaviour extends over the finite temperature range  $0 < T < T_{\text{BKT}}^{(2)}$ , without long-range order, is known as *quasi-long-range order*.

2.1. A transfer operator for the **XY** model

In this section we set up a transfer operator for the XY model, in preparation for the detailed study of its duality properties and symmetries. We assume open boundary conditions in the  $\mathbf{e}_1$ -direction and periodic ones in the  $\mathbf{e}_2$ -direction.

Since we are considering the XY model on a square lattice of size  $N \times N$  we will need the operators

$$L_{z,i} = -i \frac{\partial}{\partial \theta_i}, \quad \text{and} \quad e^{\pm i \hat{\theta}_i}, \quad i = 1, 2, \dots, N, \quad (6)$$

satisfying the following commutation relations

$$[L_{z,i}, e^{\pm i \hat{\theta}_j}] = \pm \delta_{i,j} e^{\pm i \hat{\theta}_j}. \quad (7)$$

The eigenstates of the unitary operators  $e^{\pm i \hat{\theta}_i}$ ,

$$e^{\pm i \hat{\theta}_i} |\theta_i\rangle = e^{\pm i \theta_i} |\theta_i\rangle, \quad \theta_i \in [0, 2\pi), \quad (8)$$

satisfy

$$\langle \theta'_i | \theta_i \rangle = \delta(\theta'_i - \theta_i), \quad \int_0^{2\pi} d\theta_i |\theta_i\rangle \langle \theta_i| = \mathbf{1}. \quad (9)$$

The plane wave eigenstates  $|n_i\rangle$  of  $L_{z,i}$  form an orthonormal basis of the Hilbert space of square integrable functions on the circle  $\mathcal{L}^2(\text{U}(1)) = \mathcal{H}_i$ , and are related to the states  $|\theta_i\rangle$  via  $\langle \theta_i | n_i \rangle = e^{i \theta_i n_i} / \sqrt{2\pi}$ .

On the one hand,  $e^{\pm i \hat{\theta}_i}$  represent position operators for the spin at site  $i$ , since their simultaneous eigenstates  $|\theta_i\rangle$  specify one, and only one point on the unit circle. On the other hand,  $L_{z,i}$  represents their canonically conjugate momentum, the infinitesimal generator of translations

$$e^{-i \delta L_{z,i}} |\theta_i\rangle = |\theta_i + \delta\rangle. \quad (10)$$

This last equation follows from Eq. (7), since

$$e^{i \delta L_{z,i}} e^{\pm i \hat{\theta}_i} e^{-i \delta L_{z,i}} = e^{\pm i(\hat{\theta}_i + \delta)}. \quad (11)$$

The product states,

$$|\theta\rangle = \bigotimes_i |\theta_i\rangle, \quad (12)$$

that are simultaneous eigenstates of all the position operators  $e^{\pm i\hat{\theta}_i}$ , form an orthonormal basis of the total Hilbert space  $\mathcal{H} = \bigotimes_i \mathcal{H}_i$ .

We have now all the ingredients needed to write down a transfer operator for the XY model. Consider for concreteness the following row-to-row ( $j$  to  $j + 1$ ) matrix elements of the transfer operator

$$\langle \theta' | T_2 | \theta \rangle = \exp \left[ \sum_{i=1}^N K_2 \cos(\theta_{i,j+1} - \theta_{i,j}) \right], \quad (13)$$

and the diagonal operator

$$T_1 | \theta \rangle = \exp \left[ \sum_{i=1}^{N-1} K_1 \cos(\theta_{i+1,j} - \theta_{i,j}) \right] | \theta \rangle. \quad (14)$$

Both matrices are defined in the basis of states introduced in Eq. (12). It is straightforward to check that if we set  $T_{XY} \equiv T_2 T_1$ , then

$$\text{tr} [T_{XY}^N] = \mathcal{Z}_{XY}[K_\mu, h = 0], \quad (15)$$

recovers the partition function for the XY model of Eq. (3), provided that we set the external magnetic field  $h$  to zero.

Next, we rewrite the operators  $T_1$ ,  $T_2$  in terms of the operators introduced in Eq. (7). The result reads

$$T_1 = \prod_{i=1}^{N-1} e^{K_1 \cos(\hat{\theta}_{i+1} - \hat{\theta}_i)}, \quad T_2 = \prod_{i=1}^N \int_0^{2\pi} d\theta e^{K_2 \cos \theta} e^{-i\theta L_{z,i}}, \quad (16)$$

as can be checked by taking matrix elements of  $T_2 T_1$  in the basis of Eq. (12). Notice that  $T_1$  factors into a product of two-body operators that involves only nearest neighbors, while  $T_2$  factors into a product of one-body operators. This important simplification is a direct reflection of locality.

The relevant symmetries of the classical XY model translate into unitary transformations that commute with  $T_{XY} \equiv T_2 T_1$ . Besides the obvious geometrical symmetries of the lattice,  $T_{XY}$  commute with two operators that represent internal, global symmetries. The continuous global U(1) symmetry under global rotations of the classical spin direction  $\theta_{\mathbf{r}} \rightarrow \theta_{\mathbf{r}} + \alpha$ ,  $\forall \mathbf{r}$ , guarantees that  $[L_z, T_{XY}] = 0$ , where  $L_z = \sum_{i=1}^N L_{z,i}$  is the total angular momentum. There is also a discrete symmetry  $\mathcal{C}_0 = \prod_{i=1}^N C_{0i}$  that is alluded



to, somewhat inaccurately, as “charge conjugation” [27]. The operator  $C_{0i}$  acts on position eigenstates as  $C_{0i}|\theta_i\rangle = |2\pi - \theta_i\rangle$ , and on angular momentum eigenstates as  $C_{0i}|n_i\rangle = |-n_i\rangle$ . Thus,  $C_{0i}^2 = \mathbb{1}$  and  $C_{0i}^\dagger = C_{0i}$ . Since  $\mathcal{C}_0$  does not commute but rather anticommutes with  $L_z$ , we notice that the full group of internal symmetries of the XY model is non-Abelian.

## 2.2. Hamiltonian form of the **XY** model

Models that can be written in terms of an Hermitian transfer matrix or operator, such as the XY model, can be translated into quantum-mechanical problems [11] by simply defining a quantum Hamiltonian according to

$$H_{\text{XY}} = -\ln(T_{\text{XY}}), \quad \text{or equivalently,} \quad T_{\text{XY}} = e^{-H_{\text{XY}}}. \quad (17)$$

While this is a powerful tool, often used in the literature, its actual value is diminished by the technical problem of computing  $\ln(T_{\text{XY}})$  and, perhaps more importantly, because  $H_{\text{XY}}$  turns out to be a highly non-local operator. The standard way out of this difficulty is to make approximations that solve both of these problems. The qualitative picture that emerges is intuitively appealing but problematic if the approximations are not reasonably controlled.

We will not determine  $H_{\text{XY}}$  in closed form, but rather we will compute

$$H_\mu = -\ln T_\mu, \quad \mu = 1, 2. \quad (18)$$

in closed form, and then exploit the Baker-Campbell-Hausdorff (BCH) formula to obtain the expansion

$$H \equiv -\ln(e^{-H_2}e^{-H_1}) = H_1 + H_2 + [H_1, H_2]/2 + \dots. \quad (19)$$

Since  $T_{\text{XY}} = T_2T_1$ , as defined in the previous section, is not Hermitian, we have to set  $H_{\text{XY}} = (H + H^\dagger)/2$ . This only affects terms quadratic and higher order in the commutators. We will also study the conditions for the non-diagonal (kinetic) part of the Hamiltonian  $H_2$  to reduce to the intuitively appealing form  $H_2 \propto \sum_i L_{z,i}^2/2$ .

Referring back to the operator form of  $T_1$ ,  $T_2$ , Eq. (16), we see that it is straightforward to compute  $H_1$ . Since  $T_1$  is already in diagonal form, we obtain

$$H_1 = -\sum_{i=1}^{N-1} K_1 \cos(\hat{\theta}_{i+1} - \hat{\theta}_i). \quad (20)$$

On the other hand,  $T_2$  is not diagonal. Computing  $H_2$  is further simplified by the fact that  $T_2$  factors into the product of  $N$  commuting one-body operators. It follows that  $H_2 = \sum_{i=1}^N H_{2,i}$ , with

$$e^{-H_{2,i}} = \int_0^{2\pi} d\theta e^{K_2 \cos \theta} e^{-i\theta L_{z,i}}. \quad (21)$$

Next we notice that, since  $e^{-i\theta_1 L_{z,i}} e^{-i\theta_2 L_{z,i}} = e^{-i(\theta_1+\theta_2)L_{z,i}}$ ,  $H_{2,i}$  should be of the form (see Appendix A)

$$H_{2,i} = - \int_0^{2\pi} d\theta a_{K_2}(\theta) e^{-i\theta L_{z,i}}. \quad (22)$$

By combining this expression with Eq. (21), we get an equality between functions of  $L_{z,i}$  that can be evaluated in that operator's diagonal basis. The result is an infinite set of equations

$$\int_0^{2\pi} d\theta a_{K_2}(\theta) e^{-i\theta n} = \ln(2\pi I_n(K_2)), \quad n \in \mathbb{Z}, \quad (23)$$

that one can use to determine  $a_{K_2}(\theta)$  by taking the Fourier transform of the left-hand side. The modified Bessel functions of the first kind and of integer order  $n$ ,  $I_n(K_2)$ , satisfy [28]

$$e^{K_2 \cos \theta} = \sum_{n \in \mathbb{Z}} I_n(K_2) e^{i\theta n} = I_0(K_2) + 2 \sum_{n=1}^{\infty} I_n(K_2) \cos(\theta n), \quad (24)$$

after using the relation  $I_{-n}(K) = I_n(K)$  [28].

It follows from Eq. (23) that  $a_{K_2}(2\pi - \theta) = a_{K_2}(\theta)$ , so that we can make the substitution  $e^{-i\theta L_{z,i}} \rightarrow \cos(\theta L_{z,i})$  in Eq. (22). Then, we can Taylor-expand the cosine function to get

$$H_{2,i} = - \sum_{m=0}^{\infty} a_m(K_2) L_{z,i}^{2m}, \quad (25)$$

with  $a_m(K_2) = (-1)^m \int_0^{2\pi} d\theta \theta^{2m} a_{K_2}(\theta) / (2m)!$ . This equation provides a very convenient representation of  $H_{2,i}$ , especially if we are allowed to discard terms beyond  $m = 1$ . To investigate this possibility, consider Eqs. (21) and (25), and evaluate those expressions in the  $L_{z,i}$ 's diagonal basis to get

$$\sum_{m=0}^{\infty} a_m(K_2) n^{2m} = \ln(2\pi I_n(K_2)). \quad (26)$$

For large  $K_2$ , the functions  $I_n(K_2)$  have the following asymptotic expansion [28]

$$I_n(K_2) \sim \frac{e^{K_2}}{\sqrt{2\pi K_2}} \sum_{m=0}^{\infty} (-1)^m \frac{c_m(n)}{K_2^m}, \quad (27)$$

with

$$c_0(n) = 1, \quad c_m(n) = \frac{(4n^2 - 1)(4n^2 - 3^2) \cdots (4n^2 - (2m - 1)^2)}{m! 8^m}, \quad m \geq 1. \quad (28)$$

Notice that this can be rearranged into an expansion in  $n^2$  that can be compared to the left-hand side of Eq. (26). Keeping, for each  $m$ , only the leading order in  $1/K_2$ , and expanding the logarithm accordingly ( $\ln(1+x) \sim x$ ), we obtain

$$\ln(2\pi I_n(K_2)) \sim \ln\left(\sqrt{\frac{2\pi}{K_2}} e^{K_2}\right) + \sum_{m=1}^{\infty} (-1)^m \frac{n^{2m}}{2^m m! K_2^m}. \quad (29)$$

Comparing with Eq. (26),

$$a_0(K_2) \sim \ln\left(\sqrt{\frac{2\pi}{K_2}} e^{K_2}\right), \quad a_m(K_2) \sim \frac{(-1)^m}{2^m m! K_2^m}, \quad m \geq 1, \quad (30)$$

so that  $a_{m+1}/a_m \sim -1/(2(m+1)K_2)$ . In summary, in the large  $K_2$  limit,

$$H_{\text{XY}} \approx -N a_0(K_2) + \sum_{i=1}^N \frac{1}{2K_2} L_{z,i}^2 - \sum_{i=1}^{N-1} K_1 \cos(\hat{\theta}_{i+1} - \hat{\theta}_i), \quad (31)$$

which is the one-dimensional O(2) quantum rotor model.

### 2.3. Duality of the **XY** model without the Villain approximation

We now exploit the detailed understanding we have gained on the exact operator structure of the XY model to look for its dual representations. The standard approach to the dualities of the XY model starts by replacing it with the Villain model (see Appendix C), then mapping the latter to the solid-on-solid (SoS) model, and finally mapping the SoS model to a lattice Coulomb gas [11]. In contrast, in this section we establish directly *exact* dual representations of the XY model. In Appendix B, we establish a duality to a  $q$ -deformed boson Hamiltonian which illustrates the fact that

non-canonical bosons need to emerge because of the compact nature of the degrees of freedom of the XY model.

Our methodology starts with the transfer operators  $T_1$ ,  $T_2$  introduced in Eq. (16). The algebra of interactions, or *bond algebra* in the language of Refs. [12, 13, 14, 15], underlies their basic structure. In this case, this is the von Neumann algebra  $\mathcal{A}_{XY}$  generated by the bonds

$$L_{z,1}, \quad L_{z,i}, \quad e^{\pm i(\hat{\theta}_i - \hat{\theta}_{i-1})}, \quad i = 2, \dots, N.$$

Notice that  $T_1, T_2 \in \mathcal{A}_{XY}$ , since these operators are expressible as sums of products of the bonds listed in Eq. (32).  $\mathcal{A}_{XY}$  reflects the interactions present in the XY model and is at the same time easy to characterize in terms of relations. Then we can look for other dual realizations  $\mathcal{A}_{XY}^D$  that are isomorphic images of  $\mathcal{A}_{XY}$ . By the general properties of von Neumann algebras, it must be that  $\mathcal{A}_{XY}^D = \mathcal{U}_d \mathcal{A}_{XY} \mathcal{U}_d^\dagger$ , with  $\mathcal{U}_d$  unitary, provided both algebras act on state Hilbert spaces of the same dimensionality. This is all we need to establish a duality for the XY model. The dual partition function is determined from the dual transfer operator  $T_{XY}^D = \mathcal{U}_d T_{XY} \mathcal{U}_d^\dagger$ .

The goal of this section is to look for a dual representation of the XY model in terms of integer-valued degrees of freedom, so we can expect the dual bond algebra  $\mathcal{A}_{XY}^D$  to act on the state space  $\bigotimes_{i=1}^N \mathcal{L}^2(\mathbb{Z})$ . Let us introduce the states  $|n\rangle = \bigotimes_{i=1}^N |n_i\rangle$ , and the operators  $X_i, R_i$

$$\begin{aligned} X_i |n\rangle &= n_i |n\rangle, \\ R_i |n\rangle &= |\dots, n_{i-1}, n_i - 1, n_{i+1}, \dots\rangle, \quad R_i^\dagger |n\rangle = |\dots, n_{i-1}, n_i + 1, n_{i+1}, \dots\rangle, \end{aligned} \quad (32)$$

that satisfy the algebra

$$[X_i, R_j] = -\delta_{i,j} R_j, \quad [X_i, R_j^\dagger] = \delta_{i,j} R_j^\dagger, \quad R_j R_j^\dagger = \mathbf{1}. \quad (33)$$

Then, the operators

$$X_1, \quad X_{i+1} - X_i, \quad R_i, \quad R_i^\dagger, \quad i = 1, \dots, N-1, \quad (34)$$

generate an isomorphic dual representation  $\mathcal{A}_{XY}^D$  of the bond algebra of the XY model. The isomorphism  $\Phi_d$  connecting the two bond algebras

$$\begin{aligned} L_{z,1} &\xrightarrow{\Phi_d} X_1, & L_{z,i} &\xrightarrow{\Phi_d} X_i - X_{i-1}, & i = 2, \dots, N, \\ e^{+i(\hat{\theta}_{i+1} - \hat{\theta}_i)} &\xrightarrow{\Phi_d} R_i, & e^{-i(\hat{\theta}_{i+1} - \hat{\theta}_i)} &\xrightarrow{\Phi_d} R_i^\dagger, & i = 1, \dots, N-1, \end{aligned} \quad (35)$$

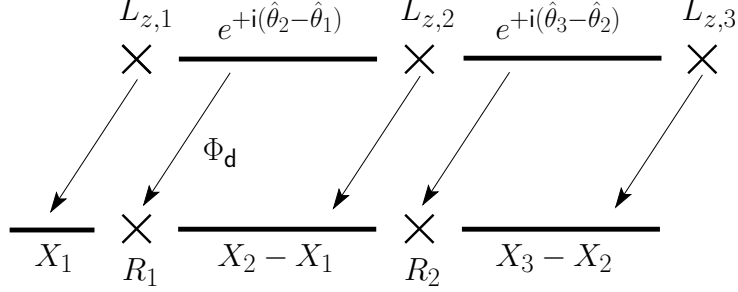


Figure 2: The bond algebra isomorphism  $\Phi_d(\cdot) = \mathcal{U}_d \cdot \mathcal{U}_d^\dagger$  defined in Eq. (35), illustrated for  $N = 3$  sites.

is illustrated in Fig. 2, for  $N = 3$  sites. The resulting dual transfer operators are

$$T_1^D = \prod_{i=1}^{N-1} e^{\frac{K_1}{2}(R_i + R_i^\dagger)}, \quad (36)$$

$$T_2^D = \int_0^{2\pi} d\theta e^{K_2 \cos \theta} e^{-iX_1} \prod_{i=2}^N \int_0^{2\pi} d\theta e^{K_2 \cos \theta} e^{-i(X_i - X_{i-1})}. \quad (37)$$

The next and last step is to compute the dual partition function

$$\mathcal{Z}_{XY}^D = \text{tr} [(T_2^D T_1^D)^N] = \text{tr} [(T_{XY}^D)^N], \quad (37)$$

in the product basis states of Eq. (32).

$T_2^D$  is already diagonal in that basis, leading simply to

$$T_2^D |n\rangle = \exp \left[ -V_{K_2}(n_{1,j}) - \sum_{i=2}^N V_{K_2}(n_{i,j} - n_{i-1,j}) \right] |n\rangle, \quad (38)$$

where

$$V_K(n) = -\ln \int_0^{2\pi} d\theta e^{K \cos \theta} e^{-i\theta n} = -\ln(2\pi I_n(K)). \quad (39)$$

The evaluation of  $\langle n' | T_1^D | n \rangle$  factors into the computation of the one-body matrix elements,

$$\langle n'_i | e^{\frac{K_1}{2}(R_i + R_i^\dagger)} | n_i \rangle. \quad (40)$$

This is simplified by noticing that the Fourier transform operator of Eq. (A.2) maps

$$F_i^\dagger R_i F_i = e^{-i\hat{\theta}_i}, \quad F_i^\dagger R_i^\dagger F_i = e^{i\hat{\theta}_i} \quad (41)$$

thus putting the exponential in diagonal form. It follows that

$$\langle n'_i | e^{\frac{K_1}{2}(R_i + R_i^\dagger)} | n_i \rangle = 2\pi e^{-V_{K_1}(n_{i,j+1} - n_{i,j})}. \quad (42)$$

If we now put all the pieces together, we arrive at the conclusion that we have obtained the exact duality

$$\frac{\mathcal{Z}_{\text{XY}}[K_\mu]}{(2\pi)^N} = \sum_{\{n_{i,j}\}} e^{[-\sum_{j=1}^N \sum_{i=1}^{N-1} (V_{K_2}(n_{i+1,j} - n_{i,j}) + V_{K_1}(n_{i,j+1} - n_{i,j})) + \sum_{j=1}^N V_{K_2}(n_{1,j})]}. \quad (43)$$

This illustrates a typical characteristic of dualities: the coupling  $K_1$  ( $K_2$ ) in the  $\mathbf{e}_1$  ( $\mathbf{e}_2$ )-direction of the XY model regulates the interaction in the orthogonal  $\mathbf{e}_2$  ( $\mathbf{e}_1$ )-direction of the dual model.

It is standard to argue that the Villain model is an excellent approximation to the XY model, specially at low temperatures. As shown in Appendix C, the Villain model is dual to the SoS model. Thus, it must be that the SoS model is approximately related to  $\mathcal{Z}_{\text{XY}}^D$  defined by the right-hand side of Eq. (43), at least for low temperatures. Consider then the limit of large  $K_1$ ,  $K_2$  (i.e., low temperatures). We can then use the asymptotic expansion of Eq. (27) to obtain an asymptotic form of the dual potential of Eq. (39),

$$V_K(n) \approx \frac{n^2}{2K} + c(K), \quad K \rightarrow \infty, \quad (44)$$

where  $c(K)$  is independent of  $n$  and can be computed from Eqs. (39) and (27). It follows that

$$\mathcal{Z}_{\text{XY}}^D \propto \sum_{\{n_{i,j}\}} e^{[-\sum_{j=1}^N \sum_{i=1}^{N-1} (n_{i+1,j} - n_{i,j})^2 / 2K_2 + (n_{i,j+1} - n_{i,j})^2 / 2K_1 + \sum_{j=1}^N (n_{1,j})^2 / 2K_2]}. \quad (45)$$

to the same level of approximation. Thus we have recovered the well known result that the XY model at very low temperatures (strong coupling) is well represented by the (approximately dual) SoS model at very high temperatures (weak coupling).

The action of the duality of Eq. (35) can be extended to act on the operator  $e^{i\hat{\theta}_N}$  as  $\Phi_d(e^{-i\hat{\theta}_N}) = R_N$ . It follows that  $\Phi_d$  generates the following set of  $N$  dual variables (below we distinguish a dual variable by an overtilde),

$$\begin{aligned} \widetilde{e^{-i\hat{\theta}_i}} &\equiv \Phi_d(e^{-i\hat{\theta}_i}) = \prod_{m=i}^N R_m, \quad i = 1, \dots, N \\ \widetilde{L_{z,1}} &\equiv \Phi_d(L_{z,1}) = X_1, \quad \widetilde{L_{z,i}} \equiv \Phi_d(L_{z,i}) = X_i - X_{i-1}, \quad i = 2, \dots, N. \end{aligned} \quad (46)$$

The dual variables satisfy the algebra of Eq. (7), confirming that  $\Phi_d$  defines an algebra isomorphism. Since this is also the algebra of the variables  $R_i, R_i^\dagger, X_i$ , we see that the dual variables  $\widetilde{e^{\pm i\hat{\theta}_i}}, \widetilde{L_{z,i}}$  afford an alternative representation of the elementary degrees of freedom. But what is their thermal behavior? This crucial question can be answered easily because  $\Phi_d$  amounts to a unitary transformation. It follows that

$$\begin{aligned} \langle e^{i\theta_{m+r,n+s}} e^{-i\theta_{m,n}} \rangle &= \frac{\text{tr} (T_{XY}^{(N-n-s)} e^{i\hat{\theta}_{m+r}} T_{XY}^s e^{i\hat{\theta}_m} T_{XY}^n)}{\mathcal{Z}_{XY}} \\ &= \frac{\text{tr} (T_{XY}^{D(N-n-s)} e^{i\hat{\theta}_{m+r}} T_{XY}^{Ds} e^{i\hat{\theta}_m} T_{XY}^n)}{\mathcal{Z}_{XY}^D} \\ &= \langle e^{i\tilde{\theta}_{m+r,n+s}} e^{-i\tilde{\theta}_{m,n}} \rangle, \end{aligned} \quad (47)$$

that should be compared to

$$\langle n_{m+r,n+s} n_{m,n} \rangle = \frac{\text{tr} (T_{XY}^{(N-n-s)} X_{m+r} T_{XY}^s X_m T_{XY}^n)}{\mathcal{Z}_{XY}^D}. \quad (48)$$

The classical dual variables  $e^{-i\tilde{\theta}_{m,n}}$  are difficult to define directly, but they are well defined in the sense that any correlator

$$\langle e^{(-1)^{\sigma_1} i\tilde{\theta}_{m_1,n_1}} e^{(-1)^{\sigma_2} i\tilde{\theta}_{m_2,n_2}} \dots e^{(-1)^{\sigma_N} i\tilde{\theta}_{m_N,n_N}} \rangle, \quad \sigma_i = 0, 1, \quad (49)$$

in the ensemble  $\mathcal{Z}_{XY}^D$  can be computed by a straightforward generalization of (47).

The duality to a lattice Coulomb gas is of a very special nature (Poisson duality) and quite different from every other duality discussed in this article (or in literature on dualities in general). Its general features are discussed in Ref. [13]. Here, we briefly summarize the exact Coulomb gas-like dual model for the exact dual partition function  $\mathcal{Z}_{XY}^D$  computed above. According to Ref. [13], the lattice gas representation of  $\mathcal{Z}_{XY}^D$  is defined by

$$\mathcal{Z}_{XY}^{DD} = \sum_{\{n_r\}} e^{-\mathcal{E}^D\{n_r\}}, \quad (50)$$

with interaction energy  $\mathcal{E}^D$  defined through the *global* Fourier transform

$$e^{-\mathcal{E}^D\{n_r\}} = \int \prod_r dx_r e^{i2\pi \sum_r n_r x_r} e^{\sum_r \sum_{\mu=1,2} V_{K_\mu}(x_r + e_\mu - x_r)}. \quad (51)$$

The interaction energy  $\mathcal{E}^D$  can be determined in closed-form in the limit in which  $\mathcal{Z}_{XY}^D$  reduces to the SoS model, and corresponds to the standard lattice Coulomb gas result [11]. We see from Eq. (51) that Poisson dualities are in general only of practical use for models with Gaussian energy functionals.

### 3. The $p$ -clock model: A close relative of XY

The  $p$ -clock model, also known as the vector Potts or  $\mathbb{Z}_p$  model, represents a hierarchy of approximations to the XY model as a function of the positive integer  $p$ , and is a test ground for rich critical behavior. In  $D = 2$  dimensions, the configurations of the classical  $p$ -clock model are described by a set of  $p$  discretized angles  $\theta_r$

$$\theta_r = \frac{2\pi s_r}{p}, \quad s_r = 0, 1, \dots, p-1. \quad (52)$$

The partition function is given by

$$\mathcal{Z}_p[K_\mu] = \sum_{\{\theta_r\}} \exp \left[ \sum_r \sum_{\mu=1,2} K_\mu \cos(\theta_{r+\mathbf{e}_\mu} - \theta_r) \right]. \quad (53)$$

This is, in appearance, identical to the classical XY model ( $h = 0$ ), except for the essential fact that the degrees of freedom  $\{\theta_r\}$  are now discrete and countable. In the large  $p$  limit ( $p \rightarrow \infty$ ), however, one supposedly recovers the XY model. Since the  $p$  points  $e^{i\theta_r}$  close a  $\mathbb{Z}_p$  subgroup of  $U(1)$  (the group of  $p$ 'th roots of unity), the  $p$ -clock model manages to provide an approximation to the XY model that features a finite number of states per site, without sacrificing the XY's natural group structure. Also like the XY model, the  $p$ -clock has interesting but hard to uncover duality properties [20]. We will address this problem by the same methods applied to the XY model. In fact, we will follow the discussion of the XY model as closely as possible, to highlight the connections between the two models.

#### 3.1. A transfer matrix for the $p$ -clock model

To introduce a transfer matrix for the  $p$ -clock model, we need to define a suitable Hilbert space and a set of basic kinematical operators. Let  $\mathcal{Z}_p$  be defined on an  $N \times N$  square lattice with open boundary conditions on the



$\mathbf{e}_1$ -direction and periodic ones on the  $\mathbf{e}_2$ -direction. The states on each site  $i = 1, \dots, N$  of a row can be described by orthonormal vectors

$$|s_i\rangle, \quad s_i = 0, \dots, p-1, \quad (54)$$

such that  $s_i$  represents the discrete angle  $2\pi s_i/p$ . They span the state space  $\mathcal{H}_{p,i}$  at site  $i$ , so the total state space is just  $\mathcal{H}_p = \bigotimes_{i=1}^N \mathcal{H}_{p,i}$ . If we write  $|s\rangle \equiv \bigotimes_{i=1}^N |s_i\rangle$  for elements of the product basis of  $\mathcal{H}_p$ , then we can define a matrix

$$\langle s'|T_2|s\rangle = \exp \left[ \sum_{i=1}^N K_2 \cos \left( \frac{2\pi s_{i,j+1}}{p} - \frac{2\pi s_{i,j}}{p} \right) \right], \quad (55)$$

related to any pair of adjacent rows  $j, j+1$ , and the diagonal matrix

$$T_1|s\rangle = \exp \left[ \sum_{i=1}^{N-1} K_1 \cos \left( \frac{2\pi s_{i+1,j}}{p} - \frac{2\pi s_{i,j}}{p} \right) \right] |s\rangle. \quad (56)$$

These definitions guarantee that  $\mathcal{Z}_p[K_\mu] = \text{tr} [(T_p)^N] = \text{tr} [(T_2 T_1)^N]$ .

The degrees of freedom of the  $p$ -clock model (at any one site of the lattice) can take any value out of a discrete, equidistant subset of points of the unit circle. To proceed in analogy to Section 2.1, we need to introduce position operators and their conjugate momenta in this discrete setting. The formalism that emerges was used extensively by Schwinger in his work on the foundations of quantum mechanics [25]. In what follows, we consider only one site (one degree of freedom), for the sake of clarity. We will consider all  $N$  sites again near the end of the section.

It is easy to restrict the position operators  $e^{\pm i\hat{\theta}}$  used for the XY model to the subset of configurations available to a *clock handle* in the  $p$ -clock model. The result is the operator  $U$  satisfying

$$U|s\rangle = \omega^s |s\rangle, \quad s = 0, \dots, p-1, \quad (57)$$

with  $\omega \equiv e^{i2\pi/p}$  representing a  $p$ th root of unity. The position operator  $U$  and its Hermitian-conjugate  $U^\dagger$  satisfy  $UU^\dagger = \mathbb{1} = U^p$ . The momentum operator  $V$  conjugate to  $U$  rotates any state counter-clockwise to its *nearest-neighbor*

$$V|0\rangle = |p-1\rangle, \quad V|1\rangle = |0\rangle, \quad \dots, \quad V|p-1\rangle = |p-2\rangle. \quad (58)$$

Momentum and position operators are represented, in  $(p \times p)$  matrix form, as

$$V = \begin{pmatrix} 0 & 1 & 0 & \cdots & 0 \\ 0 & 0 & 1 & \cdots & 0 \\ \vdots & \vdots & \vdots & & \vdots \\ 0 & 0 & 0 & \cdots & 1 \\ 1 & 0 & 0 & \cdots & 0 \end{pmatrix}, \text{ and } U = \text{diag}(1, \omega, \omega^2, \dots, \omega^{p-1}). \quad (59)$$

It follows that  $V^\dagger$  implements a clockwise rotation, and that  $VV^\dagger = \mathbb{1} = V^p$ . The fundamental algebraic relation

$$VU = \omega UV \quad (60)$$

follows directly from the definitions of  $U$  and  $V$ .

As is well known from quantum mechanics, the ordinary position operator  $\hat{x}$  and its conjugate momentum operator  $\hat{p}$  are related by a Fourier transform  $\mathcal{F}$ , a unitary transformation in the space of wave functions. Essentially the same holds for the operators  $U$ ,  $U^\dagger$  and  $V$ ,  $V^\dagger$ . The appropriate unitary transformation in this context is the discrete Fourier transform  $F$ , that in matrix form reads

$$F^\dagger = \frac{1}{\sqrt{p}} \begin{pmatrix} 1 & 1 & 1 & \cdots & 1 \\ 1 & \omega & \omega^2 & \cdots & \omega^{p-1} \\ 1 & \omega^2 & \omega^4 & \cdots & \omega^{2(p-1)} \\ \vdots & \vdots & \vdots & & \vdots \\ 1 & \omega^{p-1} & \omega^{(p-1)^2} & \cdots & \omega^{(p-1)(p-1)} \end{pmatrix}. \quad (61)$$

This is also known as Schur matrix [29]. It follows that [25]

$$FUF^\dagger = V^\dagger, \quad FVF^\dagger = U, \quad (62)$$

and so the eigenvectors of  $V$ ,  $\tilde{s} = 0, 1, \dots, p-1$ ,

$$V|\tilde{s}\rangle = \omega^{\tilde{s}}|\tilde{s}\rangle, \quad \text{with } |\tilde{s}\rangle = \frac{1}{\sqrt{p}} \sum_{s=0}^{p-1} \omega^{\tilde{s}s}|s\rangle, \quad (63)$$

are easily determined via a Fourier transform of the eigenvectors of  $U$ .

In the mathematical literature  $V$  is known as the fundamental circulant matrix. This is so as it generates the algebra of circulant matrices [26] (meaning that any circulant matrix  $C$  is of the form  $C = \sum_{m=0}^{p-1} a_m V^m$ ,  $a_m \in \mathbb{C}$ ). Together,  $U$  and  $V$  generate the full algebra of  $(p \times p)$  complex matrices [25], that we continue to call the Weyl group algebra, to emphasize that we are working with a distinguished set of generators. This shows that they constitute a convenient basis set of kinematic operators, because we can write any other operator in terms of them.

We need to re-introduce the row spatial index  $i$  to apply the technology just developed and rewrite the transfer matrices of Eqs. (56) and (55) in operator form. In what follows,  $U_i$ ,  $U_i^\dagger$ ,  $V_i$ ,  $V_i^\dagger$ , for  $i = 1, \dots, N$ , will be our basic set of operators. They *commute* at different sites, satisfy the relation (60) at any one site  $i$ , and act on the state space  $\mathcal{H}_p = \bigotimes_{i=1}^N \mathcal{H}_{p,i}$ . One then obtains

$$T_1 = \prod_{i=1}^{N-1} e^{\frac{K_1}{2}(U_{i+1}^\dagger U_i + U_{i+1} U_i^\dagger)}, \quad T_2 = \prod_{i=1}^N \sum_{m=0}^{p-1} e^{K_2 \cos(2\pi m/p)} V_i^{\dagger m}. \quad (64)$$

This last expression for  $T_2$  follows from the fact that  $\langle s'_i | V_i^{\dagger m} | s_i \rangle = 0$  unless  $s'_i - s_i \equiv m \pmod{p}$  (mod( $p$ )). It should be compared to the analogous expression for the continuum circle, Eq. (16).

### 3.2. Hamiltonian form of the $p$ -clock model

In this section we compute the Hamiltonian form of the  $p$ -clock model following the strategy of Section 2.2. We start by computing  $H_\mu = -\ln T_\mu$ ,  $\mu = 1, 2$ , with  $T_1$ ,  $T_2$  as defined in Eq. (64).

Since  $T_1$  is diagonal, we can write

$$H_1 = - \sum_{i=1}^{N-1} \frac{K_1}{2} (U_{i+1}^\dagger U_i + U_i^\dagger U_{i+1}). \quad (65)$$

$H_2 = \sum_{i=1}^N H_{2,i}$ , on the other hand, is not as easy to write down.  $H_{2,i}$  is defined as

$$e^{-H_{2,i}} = \sum_{m=0}^{p-1} e^{K_2 \cos(2\pi m/p)} V_i^{\dagger m}. \quad (66)$$

As explained in Appendix A, we can solve this equation to obtain

$$H_{2,i} = - \sum_{m=0}^{p-1} a_m(K_2) V_i^{\dagger m}, \quad (67)$$

with

$$a_m(K_2) = \frac{1}{p} \sum_{s=0}^{p-1} \cos\left(\frac{2\pi ms}{p}\right) \ln \left( \sum_{l=0}^{p-1} e^{K_2 \cos(2\pi l/p)} \cos\left(\frac{2\pi ls}{p}\right) \right). \quad (68)$$

Then, the Hamiltonian  $H_p$  for the  $p$ -clock model follows

$$H_p = - \sum_{i=1}^{N-1} \frac{K_1}{2} (U_{i+1}^\dagger U_i + U_i^\dagger U_{i+1}) - \sum_{i=1}^N \sum_{m=0}^{p-1} a_m(K_2) V_i^{\dagger m}, \quad (69)$$

provided we truncate the BCH expansion of  $\ln T_p$  to linear order (see the discussion in Section 2.2). We notice for future reference that the discrete Fourier transform  $\hat{F} = \prod_{i=1}^N F_i$  maps  $H_p \rightarrow \hat{F}^\dagger H \hat{F} = \tilde{H}_p$ , with

$$\tilde{H}_p = - \sum_{i=1}^{N-1} \frac{K_1}{2} (V_{i+1}^\dagger V_i + V_i^\dagger V_{i+1}) - \sum_{i=1}^N \sum_{m=0}^{p-1} a_m(K_2) U_i^{\dagger m}. \quad (70)$$

As discussed in Appendix A, the coefficients  $a_m(K_2)$  have simple asymptotic forms in the limit  $K_2 \rightarrow \infty$ . The corresponding approximation to  $H_p$  reads

$$H_p \approx - N a_0(K_2) - K_1 H_U - 2 a_1(K_2) H_V, \quad (71)$$

with

$$H_U = \frac{1}{2} (U_N + U_N^\dagger + \sum_{i=1}^{N-1} (U_{i+1}^\dagger U_i + U_i^\dagger U_{i+1})), \quad H_V = \frac{1}{2} \sum_{i=1}^N (V_i + V_i^\dagger), \quad (72)$$

and (see Eq. (A.12))

$$a_1(K_2) \approx e^{K_2(\cos(2\pi/p)-1)}, \quad a_0(K_2) \approx K_2. \quad (73)$$

Equation (71) shows a boundary term  $(-K_1(U_N + U_N^\dagger)/2)$  not present in Eq. (69), and that we include to make this approximation to  $H_p$  *exactly self-dual* [13].

The approximation made in going from Eq. (69) to Eq. (71), that keeps only  $V_i^\dagger$  and  $V_i^{\dagger(p-1)} = V_i$ , is reminiscent of the one introduced in Section 2.2 based on Eq. (26), whereby we replaced the operator  $\cos(\theta L_{z,i})$  for the simpler  $L_{z,i}^2$  in Eq. (31). Indeed, the two approximations coincide in the  $p \rightarrow \infty$  limit. A simple way to see this is to notice that we can realize the operator  $V_i^\dagger$  directly in the Hilbert space of the XY model as  $V_i^\dagger \rightarrow e^{-i2\pi L_{z,i}/p}$ . Then, in the limit  $p \rightarrow \infty$ ,

$$V_i + V_i^\dagger \rightarrow e^{i2\pi L_{z,i}/p} + e^{-i2\pi L_{z,i}/p} \approx 2 - (2\pi/p)^2 L_{z,i}^2. \quad (74)$$

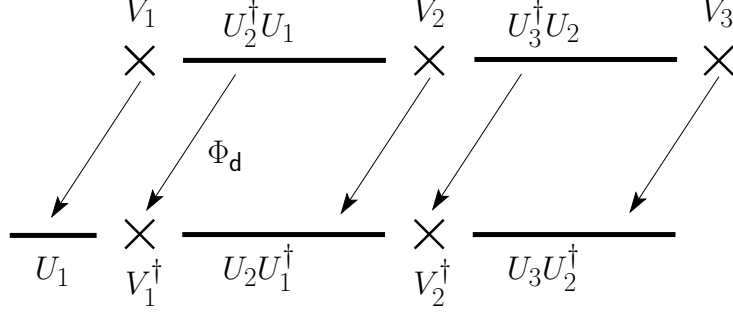


Figure 3: The duality isomorphism mapping  $\Phi_d$  of Eq. (76), for  $N = 3$  sites.

### 3.3. Dualities of the $p$ -clock model

The dualities of the  $p$ -clock model appear as isomorphic representations of the bond algebras associated to the transfer matrices defined in Eq. (64). The bond algebra  $\mathcal{A}_p$  generated by

$$V_1, V_1^\dagger, V_i, V_i^\dagger, U_i U_{i-1}^\dagger, U_i^\dagger U_{i-1}, \quad i = 2, \dots, N, \quad (75)$$

is simple to work with and adequate to our purposes. It has a dual (isomorphic) representation  $\mathcal{A}_p^D$  generated by the same bonds listed in Eq. (75), except for  $V_N, V_N^\dagger$  that have to be removed from the set of generators, and replaced by  $U_1, U_1^\dagger$ . The duality isomorphism  $\Phi_d : \mathcal{A}_p \rightarrow \mathcal{A}_p^D$  reads

$$\begin{aligned} U_{i+1}^\dagger U_i &\xrightarrow{\Phi_d} V_i^\dagger, & i = 1, \dots, N-1, \\ V_1 &\xrightarrow{\Phi_d} U_1, & V_i \xrightarrow{\Phi_d} U_{i-1}^\dagger U_i, & i = 2, \dots, N, \end{aligned} \quad (76)$$

together with the corresponding Hermitian-conjugate entries (since it must happen that  $\Phi_d(\mathcal{O}^\dagger) = \Phi_d(\mathcal{O})^\dagger$ ).  $\Phi_d$  is illustrated in Fig. 3, and should be compared with the duality of Section 2.3 for the XY model, illustrated in Fig. 2.

The dual form  $\mathcal{Z}_p^D = \text{tr} [(T_2^D T_1^D)^N]$  of the  $p$ -clock model that follows from Eq. (76) is defined by the dual transfer matrices

$$\begin{aligned} T_1^D &= \prod_{i=1}^{N-1} e^{\frac{K_1}{2}(V_i + V_i^\dagger)}, \\ T_2^D &= \sum_{m=0}^{p-1} e^{K_2 \cos(2\pi m/p)} U_1^{\dagger m} \times \prod_{i=2}^N \sum_{m=0}^{p-1} e^{K_2 \cos(2\pi m/p)} (U_i^\dagger U_{i-1})^m. \end{aligned} \quad (77)$$

Clearly, the  $p$ -clock model *is not self-dual* for arbitrary  $p$  and arbitrary couplings. However, the model is approximately self-dual in the extreme anisotropic limit with  $K_2 \gg K_1$ , and it is exactly self-dual for  $p = 2, 3, 4$ , and any coupling. We study these aspects of the  $p$ -clock model in the next sections and in Appendix D.

We mention, in closing, that there is a  $p$ -state model that approximates the  $p$ -clock in the same sense in which the Villain model approximates the XY model. This  $\mathbb{Z}_p$  Villain model [10] is exactly self-dual for any  $p$ , but is otherwise quite different from the self-dual  $p$ -clock model to be introduced next.

### 3.4. Self-dual classical $p$ -clock model

In this section we introduce a classical model  $\mathcal{Z}_{\text{sd}p}$  that we call the self-dual  $p$ -clock. It is closely related to the  $p$ -clock model (identical for  $2 \leq p \leq 4$ ), yet it is exactly self-dual for any value of  $p$ , and has the distinct advantage over the  $\mathbb{Z}_p$  Villain model [10] that its transfer matrix is remarkably simple. To define the self-dual  $p$ -clock, we introduce the transfer matrices

$$T_1[K_1] = e^{\frac{K_1}{2}(U_N + U_N^\dagger)} \prod_{i=1}^{N-1} e^{\frac{K_1}{2}(U_{i+1}^\dagger U_i + U_{i+1} U_i^\dagger)}, \quad T_2[a_0, a_1] = \prod_{i=1}^N e^{a_0 + a_1(V_i + V_i^\dagger)}. \quad (78)$$

Then,  $\mathcal{Z}_{\text{sd}p}[a_0, a_1, K_1] = \text{tr} [T_{\text{sd}p}^N]$ , with  $T_{\text{sd}p} = T_2[K_2]T_1[a_0, a_1]$ , and where  $a_0$  and  $a_1$  are free parameters of the model to be determined, for instance, by the requirement that the approximation

$$\sum_{m=0}^{p-1} e^{K_2 \cos(2\pi m/p)} V_i^{\dagger m} \approx e^{a_0 + a_1(V_i + V_i^\dagger)}, \quad (79)$$

be as good as possible for arbitrary  $K_2$ .

$\mathcal{Z}_{\text{sd}p}$  is self-dual due to the existence of a unitary transformation that maps

$$T_1[K_1] \rightarrow T_2[0, K_1], \quad T_2[a_0, a_1] \rightarrow e^{Na_0} T_1[a_1], \quad (80)$$

This fact results from a bond-algebraic analysis, but we omit the details which can be found in Ref. [13]. It follows from Eq. (80) that the self-dual line is specified by  $K_1 = 2a_1$ . The next issue then is to understand the structure of  $\mathcal{Z}_{\text{sd}p}$  in terms of classical variables. On one hand, it is clear that the interaction energy in the  $\mathbf{e}_1$ -direction is still of the form  $K_1 \cos(2\pi(s_{i+1,j} -$

$s_{i,j}/p$ ). On the other hand, the interaction energy in the  $\mathbf{e}_2$ -direction,  $u(s_{i,j} - s_{i,j+1})$ , is determined by the relation

$$\sum_{m=0}^{p-1} e^{u(m)} V_i^{\dagger m} = e^{a_0 + a_1 (V_i + V_i^\dagger)}. \quad (81)$$

Then, from Eq. (A.8),

$$e^{u(m)} = \frac{1}{[p/2]} \sum_{s=0}^{[p/2]} \cos\left(\frac{2\pi m s}{p}\right) e^{a_0 + 2a_1 \cos(2\pi s/p)} \quad (82)$$

$[p/2]$  denotes the largest integer smaller than or equal to  $p/2$ . With the interaction potential  $u$  defined in this way,

$$\mathcal{Z}_{\text{sdp}}[a_0, a_1, K_1] = \sum_{\{s_{i,j}\}} e^{\sum_{i,j} [u(s_{i,j} - s_{i,j+1}) + K_1 \cos(2\pi(s_{i+1,j} - s_{i,j})/p)]} \quad (83)$$

is exactly self-dual under the exchange  $2a_1 \leftrightarrow K_1$ .

One can see directly from Eq. (82) that  $u(p-m) = u(m)$ . It follows that

$$u(m) = \sum_{r=0}^{[p/2]} K_{2,r} \cos\left(\frac{2\pi r m}{p}\right), \quad (84)$$

with couplings

$$K_{2,r} = a_0 \delta_{r,0} + \frac{1}{[p/2]} \sum_{m=0}^{[p/2]} \cos\left(\frac{2\pi r m}{p}\right) \ln \left[ \frac{1}{[p/2]} \sum_{s=0}^{[p/2]} \cos\left(\frac{2\pi m s}{p}\right) e^{2a_1 \cos(2\pi s/p)} \right] \quad (85)$$

determined by Eq. (82) and the orthogonality relation of Eq. (A.13). The point to notice is that to make the  $p$ -clock self-dual, we need to add higher-order harmonics (terms  $\cos(2\pi m(s_{i,j} - s_{i,j+1})/p)$ , with  $m = 2, \dots, [p/2]$ ) to the basic cosine interaction. We show next that  $\mathcal{Z}_{\text{sdp}}$  becomes a very good approximation to the standard  $p$ -clock model in a suitable limit.

A comparison of the self-dual  $p$ -clock to the standard  $p$ -clock model shows that the latter has an approximate self-duality for  $p \geq 5$ . As explained in Appendix A, in the limit in which  $K_2$  is large, Eq. (79) becomes almost exact, with

$$a_0 \approx K_2, \quad a_1 \approx e^{K_2(\cos \frac{2\pi}{p} - 1)} \quad (86)$$

(see Eq. (A.12)), so that

$$\begin{aligned}
\mathcal{Z}_p[K_\mu] &\approx e^{N^2 K_2 \text{tr}} \left[ (e^{2a_1 H_V} e^{K_1 H_U})^N \right] \\
&= e^{N^2 K_2 \text{tr}} \left[ (e^{2a_1 H_U} e^{K_1 H_V})^N \right] \\
&\approx e^{N^2 (K_2 - K_2^*)} \mathcal{Z}_p[K_\mu^*]
\end{aligned} \tag{87}$$

(see Eq. (72)), with dual couplings

$$K_1^* = 2e^{K_2(\cos \frac{2\pi}{p} - 1)}, \quad K_2^* = \frac{\ln(K_1/2)}{\cos \frac{2\pi}{p} - 1}. \tag{88}$$

We emphasize that this approximate self-duality, in the extreme anisotropic limit, is valid for *any* value of  $p$ . We consider *exact* self-dualities for the particular cases  $p = 2, 3, 4$  in Appendix D.

### 3.5. Exact and emergent symmetries of the $p$ -clock model

*Non-Abelian, discrete symmetries.* The representation of the transfer matrix  $T_p = T_2 T_1$ , Eq. (64), is very convenient for understanding the internal, global symmetries of the  $p$ -clock model. It is apparent that the model has an Abelian  $\mathbb{Z}_p$  symmetry, but, as it turns out, its full group of symmetries is considerably larger and non-Abelian, provided  $p \geq 3$ . To prove this we will show that there are two Hermitian operators

$$\mathcal{C}_0 = \prod_{i=1}^N C_{0i}, \quad \mathcal{C}_1 = \prod_{i=1}^N C_{1i}, \tag{89}$$

that commute with  $T_p$  and satisfy

$$\mathcal{C}_0^2 = \mathcal{C}_1^2 = (\mathcal{C}_0 \mathcal{C}_1)^p = \mathbf{1}. \tag{90}$$

These relations show that, if  $p \geq 3$ ,  $\mathcal{C}_0$  and  $\mathcal{C}_1$  generate a unitary representation of the so called polyhedral group  $P(2, 2, p)$  [30] of order  $2p$ , and so the group of internal symmetries of the  $p$ -clock model is at least as big as this non-Abelian group. Notice that  $\mathcal{C}_0 \mathcal{C}_1 \equiv \hat{Q}$ , known as  $\mathbb{Z}_p$  charge, generates a  $\mathbb{Z}_p$  subgroup of  $P(2, 2, p)$ . This is the standard Abelian symmetry of the  $p$ -clock model that gets broken in the low-temperature ordered phase (see Section 4). It becomes a  $U(1)$  symmetry in the limit  $p \rightarrow \infty$ , and corresponds



to the usual continuous symmetry of the classical XY model  $\theta_r \rightarrow \theta_r + \alpha$ , with  $\alpha$  an arbitrary real number.

As  $\mathcal{C}_0$  and  $\mathcal{C}_1$  are products of one-site operators, let us focus on a single site  $i$  for now. We define the operators  $C_{0i}$  and  $C_{1i}$  by specifying their action on the basis of Eq. (54),

$$C_{0i}|s_i\rangle = |-s_i\rangle, \quad C_{1i}|s_i\rangle = |1-s_i\rangle, \quad s_i = 0, \dots, p-1. \quad (91)$$

The arithmetic in these definitions is modular,  $\text{mod}(p)$ . For example, if  $p = 5$ , then  $C_{0i}|0\rangle = |-0\rangle = |0\rangle$ ,  $C_{0i}|1\rangle = |-1\rangle = |4\rangle$ , and so on. Keeping this in mind, one can check that  $\mathcal{C}_0$  and  $\mathcal{C}_1$  are Hermitian,  $C_{0i}^\dagger = C_{0i}$ ,  $C_{1i}^\dagger = C_{1i}$ , and satisfy the relations listed in Eq. (90) for  $\mathcal{C}_0$  and  $\mathcal{C}_1$ . In particular, as  $C_{0i}C_{1i} = V_i$ ,  $(C_{0i}C_{1i})^p = \mathbb{1}$ . If  $p = 2$ , then  $\mathcal{C}_0 = \mathbb{1}$ , and  $\mathcal{C}_1$  generates the Abelian  $\mathbb{Z}_2$  symmetry of the Ising model which is different from the non-Abelian  $P(2, 2, 2)$ .

A routine calculation shows the action of  $C_{0i}$ ,  $C_{1i}$  on the discrete position  $U_i$  and momentum  $V_i$  operators,

$$\mathcal{C}_0 V_i \mathcal{C}_0 = V_i^\dagger, \quad \mathcal{C}_1 V_i \mathcal{C}_1 = V_i^\dagger, \quad (92)$$

$$\mathcal{C}_0 U_i \mathcal{C}_0 = U_i^\dagger, \quad \mathcal{C}_1 U_i \mathcal{C}_1 = \omega U_i^\dagger. \quad (93)$$

It is easy to check that  $\mathcal{C}_0$  and  $\mathcal{C}_1$  commute with  $T_p$ . The operator  $\mathcal{C}_0$  is known in the literature as the ‘‘charge-conjugation’’ operator [27]. However, as we alluded to earlier, this is something of a misnomer. Geometrically speaking,  $\mathcal{C}_0$  is the exact analogue of the parity operator  $\mathcal{P}|x\rangle = |-x\rangle$  on the real line. In fact,  $\mathcal{C}_0$  is related to the discrete Fourier transform as  $\hat{F}^2 = (\hat{F}^\dagger)^2 = \mathcal{C}_0$ , just as its counterpart on the real line  $\mathcal{F}$  is connected to the parity operator as  $\mathcal{F}^2 = \mathcal{P}$ .

We wish to emphasize that these non-Abelian symmetries are shared by a large number of classical and quantum  $p$ -state models besides the  $p$ -clock, including the self-dual  $p$ -clock introduced in Section 3.4 and the  $\mathbb{Z}_p$  Villain models.

*Emergent U(1) symmetry.* For  $p \geq 5$  the *discrete* charge symmetry  $\hat{Q}$  gets enhanced into a *continuous* U(1) symmetry. In reality, this is not an exact symmetry it is an *emergent* one [31], but it is essential to establish the intermediate BKT critical (massless) phase (see Section 4). Let us derive this emergent symmetry.

Given the generators of the SU(2) algebra in the spin  $S = (p-1)/2$

representation

$$\begin{aligned}
S^z &= \begin{pmatrix} \frac{p-1}{2} & 0 & 0 & \cdots & 0 & 0 \\ 0 & \frac{p-3}{2} & 0 & \cdots & 0 & 0 \\ \vdots & \vdots & \vdots & & & \vdots \\ 0 & 0 & 0 & \cdots & \frac{3-p}{2} & 0 \\ 1 & 0 & 0 & \cdots & 0 & \frac{1-p}{2} \end{pmatrix}, \\
S^+ &= \begin{pmatrix} 0 & \sqrt{p-1} & 0 & \cdots & 0 & 0 \\ 0 & 0 & \sqrt{2(p-2)} & \cdots & 0 & 0 \\ \vdots & \vdots & \vdots & & & \vdots \\ 0 & 0 & 0 & \cdots & \sqrt{2(p-2)} & 0 \\ 0 & 0 & 0 & \cdots & 0 & \sqrt{p-1} \end{pmatrix},
\end{aligned}$$

and  $S^- = (S^+)^\dagger$ , one may study the transformation properties of the Weyl's group generators  $U$  and  $V$  under the  $U(1)$  mapping

$$\mathcal{U}_\phi = e^{-i\phi S^z}. \quad (94)$$

Since  $U = \omega^{\frac{p-1}{2}} \mathcal{U}_{2\pi/p}$ , it commutes with  $\mathcal{U}_\phi$ . The transformation of  $V$  requires some thinking: Let us rewrite  $V$ , Eq. (59), as the sum of two operators

$$V = \hat{V} + \hat{\Delta}, \text{ with } \hat{\Delta} = \begin{pmatrix} 0 & 0 & 0 & \cdots & 0 \\ 0 & 0 & 0 & \cdots & 0 \\ \vdots & \vdots & \vdots & & \vdots \\ 0 & 0 & 0 & \cdots & 0 \\ 1 & 0 & 0 & \cdots & 0 \end{pmatrix}, \quad (95)$$

i.e., the matrix that has only a 1 in the lower-left corner. Then,

$$\mathcal{U}_\phi \hat{V} \mathcal{U}_\phi^\dagger = e^{-i\phi \hat{V}}, \text{ and } \mathcal{U}_\phi \hat{\Delta} \mathcal{U}_\phi^\dagger = e^{i(p-1)\phi} \hat{\Delta}. \quad (96)$$

We are interested in analyzing how the transfer matrices  $T_1$  and  $T_2$  of Eq. (64) transform under  $\hat{\mathcal{U}}_\phi = \prod_{i=1}^N \mathcal{U}_{\phi,i}$ . It is indeed easier to analyze the Fourier transform transfer matrices,  $\tilde{T}_\mu = \hat{F}^\dagger T_\mu \hat{F}$ ,

$$\tilde{T}_1 = \prod_{i=1}^{N-1} e^{\frac{K_1}{2}(V_{i+1}^\dagger V_i + V_{i+1} V_i^\dagger)}, \quad \tilde{T}_2 = \prod_{i=1}^N \sum_{m=0}^{p-1} e^{K_2 \cos(2\pi m/p)} U_i^{\dagger m}. \quad (97)$$

Clearly,  $\hat{\mathcal{U}}_\phi$  commutes with  $\tilde{T}_2$  but does not with  $\tilde{T}_1$  unless  $\phi = 2\pi/p$ , which not surprisingly corresponds to the (Fourier transform) discrete  $\hat{Q}$  symmetry. However,  $\hat{\mathcal{U}}_\phi$  is an *exact continuous* symmetry of the modified transfer matrix

$$\hat{T}_1 = \prod_{i=1}^{N-1} e^{\frac{K_1}{2}(\hat{V}_{i+1}^\dagger \hat{V}_i + \hat{V}_{i+1} \hat{V}_i^\dagger + \hat{\Delta}_{i+1}^\dagger \hat{\Delta}_i + \hat{\Delta}_{i+1} \hat{\Delta}_i^\dagger)}, \quad (98)$$

and becomes the usual U(1) symmetry of the XY model when  $p \rightarrow \infty$ . This emergent symmetry may allow for the construction of spin-wave excitations in the critical region. Note that in the original transfer matrix representation  $T_1, T_2$ , the continuous emergent symmetry is represented by  $\hat{F} \hat{\mathcal{U}}_\phi \hat{F}^\dagger$ . Moreover, it is an emergent symmetry of *both*  $p$ -clock and self-dual  $p$ -clock models.

#### 4. Phase diagram: From the $p$ -clock to the XY model

We are thus left with the task of establishing the phase diagram of the  $p$ -clock model, the nature of its phase transitions and excitations, and its behavior as  $p \rightarrow \infty$ . One may argue that the phase structure of the model is well understood [10] (see Fig. 4). At very low temperatures, there is a ferromagnetic phase characterized by long-range order of the two-point, spin-spin, correlation function  $G(|\mathbf{r} - \mathbf{r}'|) = \langle \cos(\theta_{\mathbf{r}} - \theta_{\mathbf{r}'}) \rangle$ , and the breakdown of the  $\mathbb{Z}_p$  symmetry  $\hat{Q}$ . At very high temperatures, the system is in a disordered phase with  $G(|\mathbf{r} - \mathbf{r}'|)$  decaying as an exponential function of the distance. For  $2 \leq p \leq 4$ , these two phases are separated by a continuous second-order phase transition of the Ising ( $p = 2, 4$ ) or Potts ( $p = 3$ ) type. (It is very easy to prove that the  $p = 4$  case is *identical* to two uncoupled  $p = 2$  Ising models [32], see Appendix D.) For  $p \gtrsim 5$  there is an additional intermediate *critical* phase separating the ferromagnetic from the disordered phase. It is characterized by a power-law behavior of  $G(|\mathbf{r} - \mathbf{r}'|) \sim |\mathbf{r} - \mathbf{r}'|^{-\eta}$  with a non-universal exponent  $\eta$ , and by the absence of symmetry breakdown and quasi-long-range order. In the  $p \rightarrow \infty$  limit the broken-symmetry phase disappears as one recovers the  $D = 2$  XY model with a continuous U(1) symmetry. This qualitative picture leaves several issues unresolved that numerical simulations have not been able to resolve either:

- What is the nature of the two phase transitions for  $p \gtrsim 5$ ?
- What is the nature of the relevant topological excitations in each phase?

- What is the physical origin of the critical (massless) phase?
- What is the minimum  $p$  after which the transitions are of the BKT type?

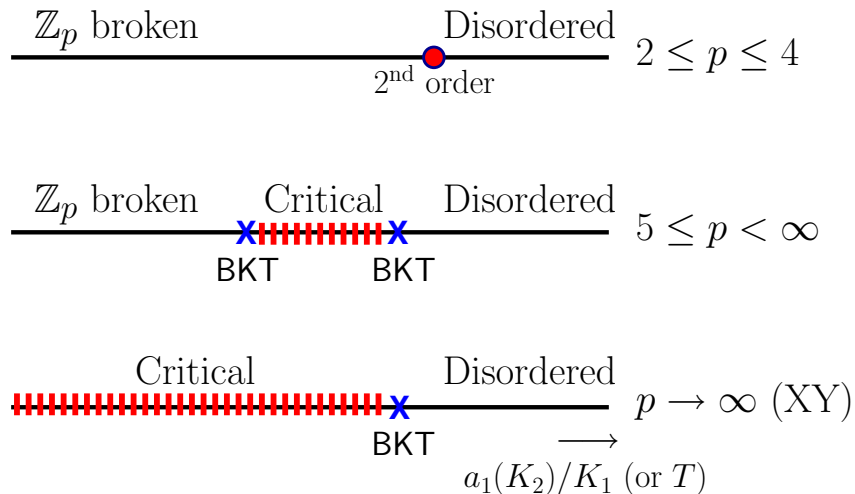


Figure 4: Phase diagram of the  $p$ -clock model. For  $p \geq 5$  there are three phases, the broken  $\mathbb{Z}_p$  (low-temperature) phase disappearing in the limit  $p \rightarrow \infty$  (XY limit). A transition is of BKT-type whenever it is associated to an essential singularity of the free energy. The critical phase is characterized by power-law correlations, i.e., quasi-long-range order, with non-universal exponents.

To understand qualitatively the nature of the phases of the model, consider the ground state of the self-dual quantum Hamiltonian  $H_p$  defined in Eq. (71), in the large (low-temperature) and small (high-temperature)  $K_1$  limits ( $a_0(K_2) = 0$ ). Let us start with the broken  $\mathbb{Z}_p$  symmetry, low temperature sector that corresponds to the line ( $K_1, a_1(K_2) = 0$ ). Then, the  $p$ -fold degenerate subspace of ground states is trivial to describe in terms of the simultaneous eigenvectors of the  $U_i$  of Eq. (57),

$$|\Psi_0^s\rangle = \prod_{i=1}^N |s_i\rangle, \quad \text{with same } s \text{ for all } i. \quad (99)$$

The ground state energy is  $E_0 = -K_1 N$  for periodic boundary conditions ( $E_0 = -K_1(N - 1)$  for open boundary conditions), and  $\langle \Psi_0^r | \Psi_0^s \rangle = \delta_{rs}$  [33].

The fully disordered, high-temperature phase is defined by the sector ( $K_1 = 0, a_1(K_2)$ ). The ground state ( $E_0 = -2a_1(K_2)N$ ) is unique and given by

$$|\Phi_0\rangle = \prod_{i=1}^N |\tilde{0}_i\rangle, \quad (100)$$

(in terms of the eigenstates of  $V_i$ , Eq. (63)), and satisfies  $\mathcal{C}_0|\Phi_0\rangle = +|\Phi_0\rangle$ . It is difficult to obtain exact results for arbitrary couplings. There is, however, an interesting exact relation that holds at the self-dual line  $K_1 = 2a_1(K_2) \equiv K^*$  and follows from the fact that the self-duality unitary  $\mathcal{U}_d$  becomes a new symmetry of the problem on that line. It is clear from Eq. (71) that  $H_p[K^*] = -K^*(H_U + H_V)$ , and  $\mathcal{U}_d H_U \mathcal{U}_d^\dagger = H_V$ ,  $\mathcal{U}_d H_V \mathcal{U}_d^\dagger = H_U$  [13]. Since  $[H_p[K^*], \mathcal{U}_d] = 0$ , we can choose the energy eigenstates  $|\Psi_n\rangle$ ,  $n = 0, 1, \dots$ , to be also eigenstates of  $\mathcal{U}_d$ ,  $\mathcal{U}_d|\Psi_n\rangle = e^{i\phi_n}|\Psi_n\rangle$ . Then

$$E_n = \langle\Psi_n|H_p[K^*]|\Psi_n\rangle = -2K^*\langle\Psi_n|H_U|\Psi_n\rangle = -2K^*\langle\Psi_n|H_V|\Psi_n\rangle. \quad (101)$$

For  $2 \leq p \leq 4$ , the  $p$ -clock model is *exactly* self-dual and the transition from the ferromagnetic to the disordered phase happens at the self-dual point  $K_1 = 2a_1(K_2)$ . For  $p \geq 5$ , Eq. (69) shows that the  $p$ -clock model is no longer exactly self-dual, but the self-dual approximation of Eq. (71) or (78) allow us to establish the following *self-dual equation* for arbitrary  $p$

$$\frac{b_1}{b_0} = e^{K_2(\cos\frac{2\pi}{p}-1)} = \frac{1}{2} \frac{\partial \ln B_p(a_1)}{\partial a_1}, \quad \text{where } B_p(a_1) = \sum_{m=0}^{p-1} e^{2a_1 \cos(\frac{2\pi}{p}m)}. \quad (102)$$

From the self-dual condition  $K_1 = 2a_1(K_2)$  one can determine the *self-dual temperature*  $T^*$ . The self-dual point is a point of non-analyticity of the free energy for  $2 \leq p \leq 4$ , but for  $p \geq 5$  it is analytic. Some values are indicated in Table 1, assuming isotropic couplings  $K_1 = K_2 = J/(k_B T)$ . It follows from very general considerations (see Section 8 of Ref. [13]) that the two critical points  $c_1$  and  $c_2$  bounding the self-dual point when  $p \geq 5$  are exactly related by

$$\left. \frac{K_1}{2a_1(K_2)} \right|_{c_1} \cdot \left. \frac{K_1}{2a_1(K_2)} \right|_{c_2} = 1. \quad (103)$$

It is interesting to analyze the large- $p$  limit of the self-dual Eq. (102). In that limit

$$\lim_{p \rightarrow \infty} \frac{1}{p} B_p(a_1) = I_0(2a_1), \quad \lim_{p \rightarrow \infty} \frac{1}{2p} \frac{\partial B_p(a_1)}{\partial a_1} = I_1(2a_1), \quad (104)$$

Table 1: Critical,  $T_c$ , and self-dual,  $T^*$ , temperatures. For  $p \geq 5$ , there are two critical temperatures. The lowest one,  $T_{\text{BKT}}^{(1)}$ , goes to zero when  $p \rightarrow \infty$ , as  $T_{\text{BKT}}^{(1)} \sim 1/p^2$ , and the highest critical temperature  $T_{\text{BKT}}^{(2)} \sim \mathcal{O}(1)$ .

$p$	$T_c$ [ $J/k_B$ ]	$T^*$ [ $J/k_B$ ]
2	$2/\ln(1 + \sqrt{2})$	$2/\ln(1 + \sqrt{2})$
3	$3/(2 \ln(1 + \sqrt{3}))$	$3/(2 \ln(1 + \sqrt{3}))$
4	$1/\ln(1 + \sqrt{2})$	$1/\ln(1 + \sqrt{2})$
6	$\dots$	$1/(2 \ln(2 \cos(\frac{\pi}{9})))$
large $p$	$\dots$	$2\pi/p$

and from the asymptotic expansion of the modified Bessel functions  $I_{0,1}$ , Eq. (27), one gets the relation between the transfer matrix and direct couplings

$$\frac{1}{2a_1(K_2)} = \frac{4\pi^2}{p^2} K_2. \quad (105)$$

One can then use Eq. (103) to obtain a relation between the two critical temperatures  $T_{\text{BKT}}^{(1)}$  and  $T_{\text{BKT}}^{(2)}$  ( $J_1 = J_2 = J$ )

$$k_B T_{\text{BKT}}^{(1)} = \frac{4\pi^2}{p^2} \frac{J^2}{k_B T_{\text{BKT}}^{(2)}}. \quad (106)$$

The Peierls argument developed in Appendix E, on the other hand, provides a rigorous scaling for the lowest transition temperature,  $T_{\text{BKT}}^{(1)} = \mathcal{O}(1/p^2)$ , as  $p \rightarrow \infty$ . Thus this lowest critical temperature vanishes for the classical XY model (where a broken-symmetry phase is not allowed) and, according to Eq. (106),  $T_{\text{BKT}}^{(2)} \sim \mathcal{O}(1)$  for large  $p$ . The self-dual temperature  $T^*$  has its own “intermediate” scaling with  $p$ ,  $k_B T^* = (2\pi/p)J$ , so that it also vanishes in the  $p \rightarrow \infty$  limit. This is to be expected since the XY model is not self-dual, nor has a natural self-dual approximation.

To understand what makes  $p \geq 5$  different from  $p < 5$  and explain the appearance of the intermediate critical phase, one needs to analyze the nature of the topological excitations. For  $p \geq 5$  there are two main types of topological excitations (see Fig. 5): (i) domain wall excitations that dominate the low-temperature physics, and (ii) discrete vortex-like excitations of relevance in the critical and high-temperature phases. The key distinction between the

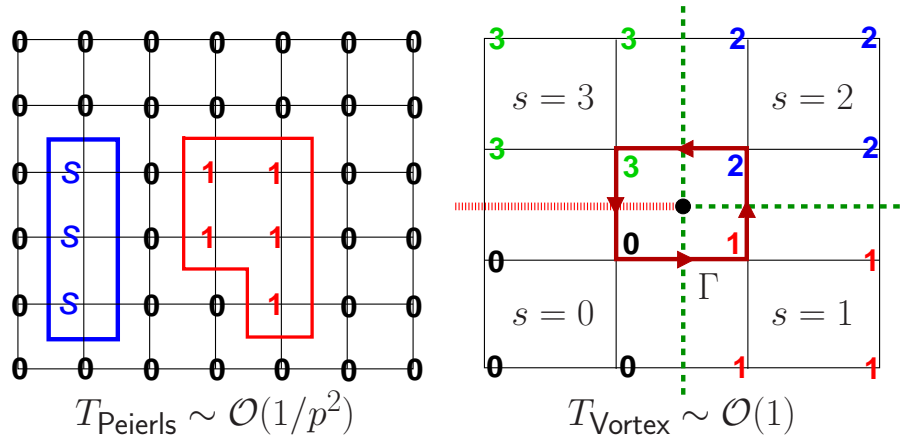


Figure 5: Two types of topological excitations: domain wall (left panel) and *discrete* vortex-like (right panel) excitations. Integer numbers  $s = 0, 1, 2, 3$  indicate the angle variables  $\theta = 2\pi s/p$ . For  $p \geq 5$  the energy cost of domain walls depends on  $|\Delta s|$  as opposed to the  $2 \leq p \leq 4$  case where the cost is independent of  $|\Delta s|$ . Vortex-like configurations start appearing at  $p = 5$ , and the example above shows a vortex in  $\mathbb{Z}_5$  of strength  $k = 1$ .

two is that domain walls exist for any  $p$ , while vortex-like excitations do not exist for  $2 \leq p \leq 4$ , becoming manifest only for  $p \geq 5$ . Also, if  $2 \leq p \leq 4$  the energy cost to create a domain wall is independent of  $|\Delta s| = |s_{\text{in}} - s_{\text{out}}|$ , with  $s_{\text{in(out)}}$  indicating the angular configurations at the two sides of the wall. This changes for  $p \geq 5$ , allowing for twists of the spin of size  $|\Delta s| = 2, \dots, (p-2)$ .

In the Peierls argument provided in Appendix E, the upper bound for the probability of having a domain wall corresponds to a change of orientation between two domains of  $(\pm 2\pi/p)$  (or equivalently  $|\Delta s| \sim \mathcal{O}(1)$ ). Such a change *always appears* in all domain walls in systems with  $p = 2, 3, 4$ . This, however, is not the case for  $p \geq 5$  where there exist general domain wall topologies that do not allow for a uniform twist of the angle between neighboring domains. In such instances,  $|\Delta s|$  can be  $\mathcal{O}(p)$  and, as shown in Fig. 5, two types of excitations are generally possible. More precisely, in  $p \geq 5$  systems, a *vorticity* arises. The topological invariant characterizing these configurations, that we call *discrete winding number*  $k$ , is given by the circulation sum

$$k = \frac{1}{2\pi} \sum_{\Gamma} \Delta\theta_{rr'}, \quad (107)$$

taken around an oriented loop  $\Gamma$ , with the argument  $\Delta\theta_{\mathbf{r}\mathbf{r}'} \in [-\pi, \pi)$  given by

$$\Delta\theta_{\mathbf{r}\mathbf{r}'} \equiv (\theta_{\mathbf{r}'} - \theta_{\mathbf{r}}) \bmod(2\pi). \quad (108)$$

In contrast, the sum in Eq. (107) *should not be taken*  $\bmod(2\pi)$  but just as an ordinary sum of real numbers (otherwise it would vanish identically). To make this definition lucid, consider a ( $p = 5$ ) configuration such as the one shown in Fig. 5, with  $\theta = 2\pi s/p$ , and a loop  $\Gamma$ . Herein, the circulation sum explicitly reads  $(\Delta\theta_{01} + \Delta\theta_{12} + \Delta\theta_{23} + \Delta\theta_{30}) = 2\pi/5 + 2\pi/5 + 2\pi/5 + 4\pi/5 = 2\pi$ . Thus, the configuration in Fig. 5 has a vortex of strength  $k = 1$  at its origin. As  $\theta_0 - \theta_3 = -6\pi/5$ , we set  $\Delta\theta_{30} = 4\pi/5$ . This shift in the value of  $\Delta\theta_{\mathbf{r}\mathbf{r}'}$  (that must lie in the interval  $[-\pi, \pi)$ ) leads to the non-zero value of  $k$  in this case.

We may now use energy-versus-entropy balance considerations to argue for the relevance of these topological excitations in establishing the two phase transitions. The Peierls argument presented in Appendix E rigorously establishes that domain walls oriented relative to one another by the minimal energy cost (i.e., twists of  $(\pm 2\pi/p)$ ) are responsible for the existence of a low-temperature ferromagnetic broken  $\mathbb{Z}_p$  symmetry phase. Both the energy penalties and entropic costs associated with such *minimal cost* domain walls scale with  $\ell$  (the domain wall length), and the analysis leads to a transition temperature that behaves as  $k_B T_{\text{BKT}}^{(1)} \sim (1 - \cos \frac{2\pi}{p})J$ . The second transition temperature,  $T_{\text{BKT}}^{(2)}$  ( $p \geq 5$ ), is associated with the proliferation of vortex-like excitations, and as indicated in Appendix E should scale as  $T_{\text{BKT}}^{(2)} \sim \mathcal{O}(1)$ . Note that this energy-versus-entropy balance argument does not rely on the existence or non-existence of the self-dual property of the model.

It is important to mention that while the physics of the low-temperature phase is associated to the exact discrete  $\mathbb{Z}_p$  symmetry, the existence of vortex-like excitations is directly related to the *emergence* of the continuous symmetry  $\hat{\mathcal{U}}_\phi$  unveiled in Section 3.5. This U(1) symmetry becomes *more exact* at high temperatures ( $T \gtrsim T^*$  or  $2a_1 \gtrsim K_1$ ), for a fixed  $p \geq 5$ , or it is exact at any temperature when  $p \rightarrow \infty$ . Thus, the physical origin of the critical phase and the *extended universality* concept introduced in Ref. [19] is simply our emergent  $\hat{\mathcal{U}}_\phi$  continuous symmetry.

What is the nature of the phase transitions when  $p \geq 5$ ? Given the current debates [22], it is important to say what we mean by a ‘‘BKT-type phase transition’’. We simply mean a transition characterized by an essential



singularity in the free energy (or the ground state energy in a quantum model). This includes those cases where there is an essential singularity but, for instance, the correlation function exponent  $\eta \neq 1/4$  ( $1/4$  is the exponent for the XY model [11]). It is very difficult to prove analytically the existence of an essential singularity but numerical simulations seem to indicate that for  $p \geq 5$  the two phase transitions are continuous with continuous derivatives [22], supporting the BKT scenario. Moreover, our new self-duality argument proves that the two transitions must be of the same nature [13]. In other words, if there is an essential singularity (the function and all its derivatives remain continuous) in the free energy at  $T_{\text{BKT}}^{(1)}$ , then, there should be the same type of singularity at  $T_{\text{BKT}}^{(2)}$  [13]. This, of course, does not mean that the self-duality fixes the value of, for instance,  $\eta$ , to be the same at the two transition points.

In what follows, we will show that when  $p \geq 5$ , the temperature region  $T_{\text{BKT}}^{(1)} \leq T \leq T_{\text{BKT}}^{(2)}$  must be critical (massless) with algebraic correlations. The assumptions are: (1) The phase transitions at  $T_{\text{BKT}}^{(1)}$  and  $T_{\text{BKT}}^{(2)}$  are continuous, and (2) for large separations  $|\mathbf{r} - \mathbf{r}'|$ , the two-point correlation function  $G(|\mathbf{r} - \mathbf{r}'|, T) = \langle \cos(\theta_{\mathbf{r}} - \theta_{\mathbf{r}'}) \rangle$  is of the canonical Ornstein-Zernike-like form

$$G(|\mathbf{r} - \mathbf{r}'|, T) \simeq A \frac{e^{-|\mathbf{r} - \mathbf{r}'|/\xi}}{|\mathbf{r} - \mathbf{r}'|^\eta} + M^2, \quad (109)$$

with  $M$  representing the order parameter, i.e., magnetization,  $\xi$  the correlation length,  $\eta$  an anomalous exponent, and  $A$  an amplitude. In principle, all of these quantities ( $M$ ,  $\xi$ ,  $\eta$ , and  $A$ ) are functions of temperature  $T$ .

We start by demonstrating that  $G(|\mathbf{r} - \mathbf{r}'|, T)$  is a monotonically decreasing function of  $T$  for any  $p$ . To this end, we derive in Appendix F a Griffiths'-type inequality as in general ferromagnetic systems [34]. Assume, for simplicity, the uniform case  $K_\mu = K > 0$ . Then, it is straightforward to show (see Appendix F) that

$$\partial_K G(|\mathbf{r} - \mathbf{r}'|, T) \geq 0, \quad (110)$$

or, equivalently,  $\partial_T G(|\mathbf{r} - \mathbf{r}'|, T) \leq 0$ , which proves that  $G$  is a monotonically decreasing function of temperature ( $0 \leq G(|\mathbf{r} - \mathbf{r}'|, T) \leq 1$ ).

Now, if  $G(|\mathbf{r} - \mathbf{r}'|, T)$  is monotonically decreasing with temperature  $T$  for any fixed separation  $|\mathbf{r} - \mathbf{r}'|$  then, in the absence of magnetization (i.e., when  $M = 0$ ) the correlation length  $\xi$  must be a monotonically decreasing function

of temperature. The proof of this assertion is trivial. Consider two rather general temperatures in this region  $T_a, T_b$ , such that  $T_{\text{BKT}}^{(1)} \leq T_a < T_b \leq T_{\text{BKT}}^{(2)}$ , then the ratio of the corresponding asymptotic correlation functions is

$$\frac{G(|\mathbf{r} - \mathbf{r}'|, T_b)}{G(|\mathbf{r} - \mathbf{r}'|, T_a)} = \frac{A_b e^{|\mathbf{r} - \mathbf{r}'|(\xi_a^{-1} - \xi_b^{-1})}}{A_a |\mathbf{r} - \mathbf{r}'|^{\eta_b - \eta_a}} \leq 1, \quad (111)$$

because of the monotonicity property of  $G$ . This is only possible if  $\xi_b < \xi_a$  for otherwise for large  $|\mathbf{r} - \mathbf{r}'|$ , the ratio of the two correlation functions would diverge exponentially in  $|\mathbf{r} - \mathbf{r}'|$ . As  $T_a$  and  $T_b$  were rather general temperatures, it follows that  $\xi(T)$  is a monotonically decreasing function of the temperature  $T$  so long as the magnetization  $M = 0$  (as it is for  $T > T_{\text{BKT}}^{(1)}$ ). Therefore, a divergence of the correlation length at  $T_{\text{BKT}}^{(1)}$  and  $T_{\text{BKT}}^{(2)}$  implies that *within the entire interval  $T_{\text{BKT}}^{(1)} \leq T \leq T_{\text{BKT}}^{(2)}$ , the correlator  $G$  is algebraic in  $|\mathbf{r} - \mathbf{r}'|$* . We thus proved that there must exist a *power law*, critical phase, between  $T_{\text{BKT}}^{(1)}$  and  $T_{\text{BKT}}^{(2)}$ .

## Acknowledgements

This work is partially supported by the National Science Foundation under Grant No. 1066293 and the hospitality of the Aspen Center for Physics. Fruitful discussions with C. D. Batista are acknowledged.

## Appendix A. Exponential of shift operators

In this appendix we collect some useful formulas to compute exponentials and logarithms of shift operators. Let us start with the operator  $L_z$ , the infinitesimal generator of translations on the circle. We have the general relation

$$e^{\int_0^{2\pi} d\theta a(\theta) e^{-i\theta L_z}} = \int_0^{2\pi} d\theta b(\theta) e^{-i\theta L_z}. \quad (A.1)$$

Our goal is to compute  $a$  as a function of  $b$ , and *vice versa*. The first step is to notice that the Fourier transform operator

$$F = \sum_{n \in \mathbb{Z}} \int_0^{2\pi} d\theta \frac{e^{-i\theta n}}{\sqrt{2\pi}} |n\rangle \langle \theta|, \quad (A.2)$$

puts  $L_z$  (and the expression of Eq. (A.1)) in diagonal form,

$$F e^{-i\theta L_z} F^\dagger = \sum_{n \in \mathbb{Z}} |n\rangle \langle n| e^{-i\theta n}. \quad (A.3)$$

This, together with the orthogonality relation  $2\pi\delta(\theta' - \theta) = \sum_{n \in \mathbb{Z}} e^{i(\theta' - \theta)n}$ , leads to

$$b(\theta) = \frac{1}{2\pi} \sum_{n \in \mathbb{Z}} e^{i\theta n} e^{\int_0^{2\pi} d\theta' a(\theta') e^{-i\theta' n}}, \quad (\text{A.4})$$

$$a(\theta) = \frac{1}{2\pi} \sum_{n \in \mathbb{Z}} e^{i\theta n} \ln \left( \int_0^{2\pi} d\theta' b(\theta') e^{-i\theta' n} \right). \quad (\text{A.5})$$

In Section 3.1 we introduced a diagonal matrix  $U$ , and a shift operator  $V^\dagger$  that describes translations in a  $p$ -points discretization of the circle. This shift operator plays a role similar to that of  $L_z$  (actually,  $e^{-i\theta L_z}$ ). Now we have the general relation

$$e^{\sum_{m=0}^{p-1} a_m V^m} = \sum_{m=0}^{p-1} b_m V^{\dagger m}, \quad (\text{A.6})$$

that should be compared to Eq. (A.1). Our goal is to find closed-form expressions for the coefficients  $a_m$  in terms of  $b_m$  and *vice versa*. The unitary transformation that diagonalizes  $V^\dagger$  is now given by the *discrete* Fourier transform of Eq. (62). Putting these pieces together, we get the solution to our problem,

$$b_m = \frac{1}{p} \text{tr} \left[ U^m e^{\sum_{l=0}^{p-1} a_l U^{\dagger l}} \right], \quad a_m = \frac{1}{p} \text{tr} \left[ U^m \ln \left( \sum_{l=0}^{p-1} b_l U^{\dagger l} \right) \right]. \quad (\text{A.7})$$

As seen by expanding the trace, these equations are closely related to (A.4) and (A.5).

In physical applications, the  $a_m$  are Hermitian-symmetric,  $a_{p-m} = a_m^*$  (to guarantee that  $\sum_{m=0}^{p-1} a_m V^m$  is a Hermitian operator), and the  $b_m$  are real and positive. Thus, it is convenient to assume that both set of coefficients satisfy  $a_{p-m} = a_m$ ,  $b_{p-m} = b_m$ , and the relations between them simplify to

$$b_m = \frac{1}{p} \sum_{s=0}^{p-1} \cos\left(\frac{2\pi m s}{p}\right) e^{\sum_{l=0}^{p-1} a_l \cos\left(\frac{2\pi l s}{p}\right)}, \quad (\text{A.8})$$

$$a_m = \frac{1}{p} \sum_{s=0}^{p-1} \cos\left(\frac{2\pi m s}{p}\right) \ln \left( \sum_{l=0}^{p-1} b_l \cos\left(\frac{2\pi l s}{p}\right) \right). \quad (\text{A.9})$$

These are the expressions that are most useful in physical applications.

Suppose next that  $b_m = e^{Ku(m)}$ , where  $K$  is a positive constant, and  $u(m)$  is a real function of  $m = 0, \dots, p-1$  (for example,  $u(m) = \cos(\frac{2\pi m}{p})$  for the classical  $p$ -clock model). We would like to study the behaviour of the  $a_m$  to next-to-leading order in  $K$ , in the limit that  $K$  grows very large (this could happen at low temperature). Notice that in this limit

$$\sum_{l=0}^{p-1} b_l \cos\left(\frac{2\pi ls}{p}\right) \approx e^{Ku(0)} \left(1 + 2e^{K(u(1)-u(0))} \cos\left(\frac{2\pi s}{p}\right)\right) \quad (\text{A.10})$$

to next-to-leading order, assuming that the inequalities

$$0 > (u(1) - u(0)) > (u(2) - u(0)) > \dots \quad (\text{A.11})$$

hold. The factor two in Eq. (A.10) is due to the symmetry  $u(p-l) = u(l)$ . Replacing expansion (A.10) into Eq. (A.8) leads to

$$a_m \approx Ku(0)\delta_{m,0} + e^{K(u(1)-u(0))}(\delta_{m,1} + \delta_{m,p-1}), \quad K \rightarrow \infty, \quad (\text{A.12})$$

where we have used  $\ln(1+x) \approx x$ , and the orthogonality relation

$$\frac{1}{p} \sum_{s=0}^{p-1} \cos\left(\frac{2\pi ms}{p}\right) \cos\left(\frac{2\pi sl}{p}\right) = \frac{1}{2} (\delta_{m,l} + \delta_{m,p-l}). \quad (\text{A.13})$$

## Appendix B. Duality of the XY model to $q$ -deformed bosons

In this section we study a duality that illustrates the essential differences between compact,  $\hat{\theta}$ , and non-compact,  $\hat{x}$ , degrees of freedom. The algebraic tool of choice is the  $q$ -oscillator algebra [35], specified by a positive real number  $q$ , a creation operator  $a^\dagger$ , its Hermitian conjugate  $a$ , and a Hermitian operator  $\hat{n}$ , satisfying

$$[\hat{n}, a] = -a, \quad [\hat{n}, a^\dagger] = a^\dagger, \quad aa^\dagger - qa^\dagger a = q^{-\hat{n}}. \quad (\text{B.1})$$

If  $q = 1$ , this algebra reduces to the standard harmonic oscillator algebra, that is isomorphic to the Heisenberg algebra of translations on the line,  $[\hat{x}, \hat{p}] = i$ , provided  $a = (\hat{x} + i\hat{p})/\sqrt{2}$ ,  $a^\dagger = (\hat{x} - i\hat{p})/\sqrt{2}$ . It was pointed out in Ref. [36] that the mapping

$$\begin{aligned} L_z &\mapsto -\hat{n} + \ln \sqrt{2 \sinh(1)}, \\ e^{i\hat{\theta}} &\mapsto \sqrt{2 \sinh(2)} a e^{-\hat{n}}, \quad e^{-i\hat{\theta}} \mapsto \sqrt{2 \sinh(2)} e^{-\hat{n}} a^\dagger, \end{aligned} \quad (\text{B.2})$$

affords a representation of the algebra of translations in the circle  $[L_z, e^{\pm i\hat{\theta}}] = \pm e^{\pm i\hat{\theta}}$ , provided that we set  $q = e^{-2}$  in Eq. (B.1).

Clearly, we can extend the mapping of Eq. (B.2) to a duality isomorphism  $\Phi_d$  for the XY model. The dual transfer operators read

$$\begin{aligned} T_2^D &= \prod_{i=1}^N \sqrt{2 \sinh(1)} \int_0^{2\pi} d\theta e^{K_2 \cos \theta} e^{i\theta \hat{n}_i}, \\ T_1^D &= \prod_{i=1}^{N-1} \exp \left[ K_1 \sinh(2) (a_{i+1} e^{-(\hat{n}_{i+1} + \hat{n}_i)} a_i^\dagger + \text{h.c.}) \right]. \end{aligned} \quad (\text{B.3})$$

To compute  $\mathcal{Z}_{\text{XY}}^D$ , one should take the trace in the eigenbasis of  $\hat{n}_i$ . This basis is described in Ref. [35].

This description of the XY model in terms of  $q$ -deformed bosons with  $q = e^{-2}$  suggests that the algebra of Eq. (B.1) affords a continuous interpolation between the XY model and ordinary phonons (characterized by  $q = 1$ ), but this is not the case: The XY model belongs to a representation of the algebra of Eq. (B.1) that is inequivalent to that describing phonons (i.e., canonical bosons). The reason is that Eq. (7) is not enough to specify the algebra of translations in the circle. We must also have that

$$e^{\pm i\hat{\theta}} e^{\mp i\hat{\theta}} = \mathbb{1}. \quad (\text{B.4})$$

The mapping of Eq. (B.2) will respect this constraint only if  $a, a^\dagger$  satisfy

$$aa^\dagger - q^{-1}a^\dagger a = 0 \quad (\text{B.5})$$

at least for  $q = e^{-2}$ , including the relations listed in Eq. (B.1). But the resulting set of four relations becomes inconsistent at  $q = 1$ . This shows that the  $q$ -oscillator algebra cannot interpolate continuously between canonical bosons and compact excitations.

## Appendix C. The Villain and its dual solid-on-solid models

The Villain model [11]

$$\mathcal{Z}_V[K_\mu] = \sum_{\{n_{(\mathbf{r}, \mu)}\}} \sum_{\{\theta_{\mathbf{r}}\}} \exp \left[ \sum_{\mathbf{r}} \sum_{\mu=1,2} \frac{K_\mu}{2} (\theta_{\mathbf{r}+\mathbf{e}_\mu} - \theta_{\mathbf{r}} - 2\pi n_{(\mathbf{r}, \mu)})^2 \right], \quad (\text{C.1})$$

was introduced in Ref. [16] to provide a Gaussian approximation to the XY model that preserves the essential property of compacticity, and is a good approximation at sufficiently low temperatures. We now show, by using our bond-algebraic approach, that it is dual to the solid-on-solid (SoS) model of the roughening transition,

$$\mathcal{Z}_{\text{SoS}}[K_\mu] = \sum_{\{m_{\mathbf{r}}\}} \exp \left[ \sum_{\mathbf{r}} \sum_{\mu=1,2} K_\mu^{-1} (m_{\mathbf{r}+\mathbf{e}_\mu} - m_{\mathbf{r}})^2 \right], \quad (\text{C.2})$$

characterized by integer-valued degrees of freedom  $m_{\mathbf{r}} \in \mathbb{Z}$  [11]. We work directly in the thermodynamic limit,  $N \rightarrow \infty$ , to avoid dealing with boundary terms.

The transfer operator  $T_{\text{SoS}} = T_2 T_1$  for the SoS model can be written as

$$T_1 = \prod_i e^{\frac{K_1}{2}(X_{i+1}-X_i)^2}, \quad T_2 = \prod_i \sum_m e^{\frac{K_2}{2}m^2} R_i^\dagger m, \quad (\text{C.3})$$

in terms of the operators  $X_i$ ,  $R_i$ ,  $R_i^\dagger$  defined in Eq. (32). Now, however,  $i \in \mathbb{Z}$  labels the sites of an infinite straight line. The duality of bond algebras

$$X_i - X_{i-1} \xrightarrow{\Phi_d} L_{z,i}, \quad R_i \xrightarrow{\Phi_d} e^{i(\hat{\theta}_{i+1}-\hat{\theta}_i)}, \quad R_i^\dagger \xrightarrow{\Phi_d} e^{-i(\hat{\theta}_{i+1}-\hat{\theta}_i)} \quad (\text{C.4})$$

affords a dual representation of  $T_{\text{SoS}}$ ,

$$T_1^D = \prod_i e^{\frac{K_1}{2}L_{z,i}^2}, \quad T_2^D = \prod_i \sum_m e^{\frac{K_2}{2}m^2} e^{-i(\hat{\theta}_{i+1}-\hat{\theta}_i)m}, \quad (\text{C.5})$$

in terms of compact degrees of freedom. The next step is to compute  $\mathcal{Z}_{\text{SoS}}^D = \text{tr} [(T_2^D T_1^D)^N]$  in the basis introduced in Eq. (9).

$T_2^D$  is already diagonal in that basis

$$T_2^D |\theta\rangle = \prod_i \sum_m e^{\frac{K_2}{2}m^2} e^{-i(\theta_{i+1,j}-\theta_{i,j})m} |\theta\rangle. \quad (\text{C.6})$$

At this point we could proceed by analogy to previous sections and rewrite this expression in terms of an interaction potential  $V_K(\theta) \equiv -\ln \sum_m e^{\frac{K_2}{2}m^2} e^{-i\theta m}$ , but this will not turn out to be the most convenient approach. Instead, let us proceed to compute the matrix elements of  $T_1^D$ . This task reduces to computing the matrix elements of a one-body operator,

$$\langle \theta'_i | \frac{K_1}{2} L_{z,i}^2 | \theta_i \rangle = \frac{1}{2\pi} \sum_{m_i} e^{\frac{K_1}{2}m_i^2} e^{-i(\theta'_i-\theta_i)m_i}, \quad (\text{C.7})$$

which results from recalling that the orthonormal states of  $L_{z,i}$  are the plane waves  $\langle \theta_i | n_i \rangle = e^{i\theta_i n_i} / \sqrt{2\pi}$ . Notice that the function  $e^{\frac{K}{2}x^2}$  is the Fourier transform of  $e^{\frac{x^2}{2K}} / \sqrt{K}$ . It then follows that we can use Poisson's summation formula to write

$$\sum_{m_i} e^{\frac{K}{2}m_i^2} e^{-i\theta m_i} = \sqrt{\frac{2\pi}{K}} \sum_{m_i} e^{\frac{(\theta - 2\pi m_i)^2}{2K}}. \quad (\text{C.8})$$

Putting all the pieces together, we obtain

$$\begin{aligned} \mathcal{Z}_{\text{SoS}}^D &= \left( \frac{2\pi}{K_2} \right)^N \sum_{\{\theta_r\}} \prod_{\mathbf{r}} \prod_{\mu=1,2} \sum_m \exp \left[ \frac{K_\mu}{2} (\theta_{\mathbf{r}+\mathbf{e}_\mu} - \theta_{\mathbf{r}} - 2\pi m)^2 \right] \\ &= \left( \frac{2\pi}{K_2} \right)^N \sum_{\{n_{(\mathbf{r},\mu)}\}} \sum_{\{\theta_r\}} \exp \left[ \sum_{\mathbf{r}} \sum_{\mu=1,2} \frac{K_\mu}{2} (\theta_{\mathbf{r}+\mathbf{e}_\mu} - \theta_{\mathbf{r}} - 2\pi n_{(\mathbf{r},\mu)})^2 \right]. \end{aligned} \quad (\text{C.9})$$

The last expression is exactly  $(2\pi/K_2)^N \mathcal{Z}_V[K_\mu]$ , and thus the Villain model is dual to the SoS model. Notice the reciprocal relation between the couplings: The Villain model is strongly coupled only if its dual SoS representation is weakly coupled.

#### Appendix D. The $p$ -clock model for $p = 2, 3$ , and 4

Let us start with the simplest  $p = 2$  case. Then,  $U_i = U_i^\dagger = \sigma_i^z$  and  $V_i = V_i^\dagger = \sigma_i^x$ , and the transfer matrix  $T_p = T_2 T_1$  of Eq. (64) reduces to

$$T_1 = \prod_{i=1}^{N-1} e^{K_1 \sigma_i^z \sigma_{i+1}^z}, \quad T_2 = \prod_{i=1}^N (e^{K_2} + e^{-K_2} \sigma_i^x). \quad (\text{D.1})$$

This finite Ising model is self-dual *up to boundary corrections*. The substitution  $T_1 \rightarrow e^{K_1 \sigma_N^z} T_1$  renders the model *exactly* self-dual for any  $N$  [13].

If  $p = 3$ , then  $V_i^{\dagger 2} = V_i$ , and  $T_2$  becomes

$$T_2 = \prod_{i=1}^N \left( e^{K_2} + e^{-\frac{K_2}{2}} (V_i + V_i^\dagger) \right). \quad (\text{D.2})$$

$T_1$  is just as in Eq. (64), with  $U$ s appropriate for  $p = 3$ . It follows that if we introduce the boundary correction  $T_1 \rightarrow e^{\frac{K_1}{2}(U_N + U_N^\dagger)} T_1$  [13], then  $T_2 \xrightarrow{\Phi_d} T_1$  and  $T_1 \xrightarrow{\Phi_d} T_2$ , rendering  $\mathcal{Z}_p$  exactly self-dual for any  $N$ .

The case  $p = 4$  is special because it can be mapped onto two decoupled Ising models [32]. Since  $V_i^2 = V_i^{\dagger 2}$  in this case,  $T_2$  reads

$$T_2 = \prod_{i=1}^N (e^{K_2} + V_i + V_i^{\dagger} + e^{-K_2} V_i^2). \quad (\text{D.3})$$

Moreover, it is easy to check that the operator  $2\mathbf{C}_i = (\mathbb{1} + \sigma_{1,i}^z) + (\mathbb{1} - \sigma_{1,i}^z)\sigma_{2,i}^x$  (known as a controlled-NOT gate in quantum computation) maps

$$\begin{aligned} U_i &= e^{i\frac{\pi}{4}} \mathbf{C}_i \left( \frac{\sigma_{1,i}^z - i\sigma_{2,i}^z}{\sqrt{2}} \right) \mathbf{C}_i, \\ V_i + V_i^{\dagger} &= \mathbf{C}_i (\sigma_{1,i}^x + \sigma_{2,i}^x) \mathbf{C}_i, \quad V_i^2 = \mathbf{C}_i \sigma_{1,i}^x \sigma_{2,i}^x \mathbf{C}_i, \end{aligned} \quad (\text{D.4})$$

and thus it follows that  $\mathbf{C} = \prod_{i=1}^N \mathbf{C}_i$  maps

$$\mathbf{C} T_1 \mathbf{C} = \prod_{i=1}^{N-1} e^{\frac{K_1}{2} (\sigma_{1,i}^z \sigma_{1,i+1}^z + \sigma_{2,i}^z \sigma_{2,i+1}^z)}, \quad (\text{D.5})$$

$$\mathbf{C} T_2 \mathbf{C} = \prod_{i=1}^N (e^{\frac{K_2}{2}} + e^{-\frac{K_2}{2}} \sigma_{1,i}^x) (e^{\frac{K_2}{2}} + e^{-\frac{K_2}{2}} \sigma_{2,i}^x), \quad (\text{D.6})$$

that clearly defines two decoupled Ising models, with couplings that are half of those of the  $p = 2$  model. In particular, the  $p = 4$  clock model is exactly self-dual provided  $T_1 \rightarrow e^{\frac{K_1}{2} (\sigma_{1,N}^z + \sigma_{2,N}^z)} T_1$ .

## Appendix E. Peierls argument for the $p$ -plock model

We now use the Peierls argument to prove that there should be a broken symmetry phase (low-temperature ordered phase) in the  $p$ -clock model on the square lattice. The proof establishes the existence of a phase transition at a temperature  $T^{(1)}$  below which global  $\mathbb{Z}_p$  symmetry is broken. For large  $p \gg 1$ ,  $T^{(1)} = \mathcal{O}(1/p^2)$ .

Specifically, our objective is to show that if uniform boundary conditions pertaining to one of the clock states  $\theta = 2\pi s/p$ , with  $0 \leq s \leq p-1$  a fixed integer, are applied on the boundary of the square lattice, then there *provably* exists a temperature  $T_{\text{Peierls}} > 0$  such that for temperatures  $T < T_{\text{Peierls}}$ , spontaneous symmetry breaking (SSB) of the global  $\mathbb{Z}_p$  symmetry arises. (In the context of our discussions thus far,  $T_{\text{Peierls}} < T^{(1)}$ ; asymptotically, for



large  $p$ , both temperatures scale as  $1/p^2$ .) By SSB in this context, we refer to the lifting of the symmetry triggered by applying the uniform boundary conditions at spatial infinity. That is, when the aforementioned boundary conditions are introduced then, for  $T < T_{\text{Peierls}}$ , the probability distribution  $\mathcal{P}(\theta_{\mathbf{0}})$  for the angular orientation of the spin at the origin  $\mathbf{S}_{\mathbf{0}}$  is not symmetric between the  $p$  possible values of  $\theta_{\mathbf{0}}$ . In particular, we will demonstrate that  $\mathcal{P}(\theta_{\mathbf{0}})$  is maximal when  $\theta_{\mathbf{0}}$  has an orientation that matches that on the boundary,  $\theta_{\infty}$ . In other words, for temperatures  $T < T_{\text{Peierls}}$ ,

$$\mathcal{P}(\theta_{\mathbf{0}} = \theta_{\infty}) \geq \frac{1}{p}. \quad (\text{E.1})$$

To prove this inequality, we note that

$$\mathcal{P}(\theta_{\mathbf{0}} \neq \theta_{\infty}) \leq \text{Prob}(\text{outer domain wall } \Gamma), \quad (\text{E.2})$$

where  $\text{Prob}(X)$  denotes the probability of the set of events  $X$ . The *domain wall* is defined as the boundary between differently oriented spins. The logic underlying Eq. (E.2) is clear: if  $\theta_{\mathbf{0}} \neq \theta_{\infty}$  then, by its very definition, at least one domain wall must separate the spin at the origin from the spins on the boundaries of the lattice.

We now will bound the probability of having a particular domain wall. Specifically, let us denote by  $\{C_{\alpha}\}$  the set of configurations that have  $\Gamma$  as the outer-most domain wall surrounding the origin. That is,  $\Gamma$  separates spins with an orientation  $\theta = \theta_{\infty}$  from those having another (uniform) orientation  $\theta_{\text{in}}$ . [Note that, generally, more than one domain wall may be present and thus  $\theta_{\text{in}}$  need not be the same as  $\theta_{\mathbf{0}}$ .] The upper bound on the probabilities in Eq. (E.2) is a sum over the probabilities of having such different outer-most domain walls  $\Gamma$ . We furthermore define the partition function

$$\mathcal{Z}_{\Gamma} = \sum_{\{C_{\alpha}\}} \exp[-\beta E_{\alpha}], \quad (\text{E.3})$$

where  $E_{\alpha} \equiv E(C_{\alpha})$  is the energy of the spin configuration  $C_{\alpha}$ . Thus,  $\mathcal{Z}_{\Gamma}$  is smaller than the total partition function  $\mathcal{Z}_p$  of the system. This is so as  $\mathcal{Z}_{\Gamma}$  contains only a subset of the Boltzmann weights appearing in  $\mathcal{Z}_p$ . That is, in Eq. (E.3) we sum only over spin configurations with at least one domain wall surrounding the origin.

We next define a new configuration  $\bar{C}_{\alpha}$  formed by rotating all of the spins inside  $\Gamma$  by a uniform angle  $\Delta\theta$  such that the outermost domain wall that

surrounds the origin is removed. That is, for all spins  $\mathbf{S}_r$  that (i) lie inside the region bounded by the domain wall  $\Gamma$ , we perform the transformation  $\theta_r \rightarrow (\theta_r + \Delta\theta)$  with an angle of rotation

$$\Delta\theta = \theta_\infty - \theta_{\text{in}} \equiv \frac{2\pi}{p}\Delta s, \quad (\text{E.4})$$

where  $\Delta s$  is an integer. (ii) All spins lying outside the domain wall  $\Gamma$  have an orientation  $\theta = \theta_\infty$ ; these spins are not rotated. When present, any other more internal domain walls will remain unchanged by this uniform rotation of all the spins inside  $\Gamma$ . In order to bound, from above, the probability of having an outermost domain wall  $\Gamma$ , we now consider ( $E_{\bar{\alpha}} = E(\bar{C}_\alpha)$ )

$$\mathcal{Z}_{\bar{\Gamma}} = \sum_{\{\bar{C}_\alpha\}} \exp[-\beta E_{\bar{\alpha}}]. \quad (\text{E.5})$$

The probability of having the domain wall  $\Gamma$  is fixed by the ratio of the sum of Boltzmann weights associated with having the domain wall  $\Gamma$  divided by the sum of Boltzmann weights associated with all spin configurations (i.e., the partition function  $\mathcal{Z}_p$ ). As  $\mathcal{Z}_{\bar{\Gamma}}$  contains a sum only over a subset of all Boltzmann weights that appear in  $\mathcal{Z}_p$ , we have

$$\text{Prob}(\text{outer domain wall } \Gamma) = \frac{\mathcal{Z}_{\bar{\Gamma}}}{\mathcal{Z}_p} \leq \frac{\mathcal{Z}_{\bar{\Gamma}}}{\mathcal{Z}_{\bar{\Gamma}}} = \frac{e^{-\beta E_{C_1}} + e^{-\beta E_{C_2}} + \dots}{e^{-\beta E_{\bar{C}_1}} + e^{-\beta E_{\bar{C}_2}} + \dots}. \quad (\text{E.6})$$

The smallest energy difference between a configuration  $C_\alpha$  and  $\bar{C}_\alpha$  is bounded by

$$E_{C_\alpha} - E_{\bar{C}_\alpha} \geq \ell(1 - \cos \frac{2\pi}{p}), \quad (\text{E.7})$$

where  $\ell$  is the length of the domain wall  $\Gamma$  (exchange constants are set to unity,  $J_\mu = 1$ ,  $\mu = 1, 2$ ). As Eq. (E.7) applies to all configuration pairs  $C_\alpha$  and  $\bar{C}_\alpha$  that appear in Eq. (E.6),

$$\frac{e^{-\beta E_{C_\alpha}}}{e^{-\beta E_{\bar{C}_\alpha}}} = e^{-\beta\ell(1 - \cos \frac{2\pi\Delta s}{p})} \leq e^{-\beta\ell(1 - \cos \frac{2\pi}{p})}, \quad (\text{E.8})$$

we have that

$$\frac{\mathcal{Z}_{\bar{\Gamma}}}{\mathcal{Z}_{\bar{\Gamma}}} \leq e^{-\beta\ell(1 - \cos \frac{2\pi}{p})}. \quad (\text{E.9})$$

It is important to emphasize that when the bound of Eq. (E.9) is saturated,  $|\Delta s| = 1$ . [Physically, for  $p \gg 1$ , only such domain walls (as opposed to far more energetically prohibitive domain walls with  $|\Delta s| = \mathcal{O}(p)$ ) may appear at sufficiently low temperatures ( $T \lesssim \mathcal{O}(1/p^2)$ ).]

Returning to the probability that (at least) one domain wall surrounds the origin in Eq. (E.2), we have that

$$\text{Prob}(\text{outer domain wall } \Gamma) \leq \sum_{\ell} N_{\ell} D_{\ell}, \quad (\text{E.10})$$

with  $N_{\ell}$  denoting an upper bound on the number of domain walls of perimeter  $\ell$  that enclose the origin and  $D_{\ell}$  an upper bound on the probability of having a domain wall of length  $\ell$ . Inserting Eq. (E.9) while taking note of an upper bound of  $4 \times 3^{\ell-1}$  on the number of non-backtracking walks of length  $\ell$  on the square lattice, and an upper bound of  $(\ell/4)^2$  on the maximum number of initial starting points for a walk of length  $\ell$  that surrounds the origin, we have

$$\begin{aligned} \text{Prob}(\text{outer domain wall } \Gamma) &\leq \sum_{\ell \geq 4} \left[ (\ell/4)^2 \times 4 \times 3^{\ell-1} e^{-\beta \ell (1 - \cos \frac{2\pi}{p})} \right] \\ &\equiv w(\beta, p) \end{aligned} \quad (\text{E.11})$$

(the minimal domain wall on the square lattice has length  $\ell = 4$ ). The function  $w$  is trivially bounded by performing the summation over all natural numbers  $\ell$

$$w(\beta, p) \leq \sum_{\ell=1}^{\infty} \frac{3^{\ell} \ell^2}{12} e^{-\beta \ell (1 - \cos \frac{2\pi}{p})} = \frac{x(1+x)}{12(x-1)^3} \equiv \bar{w}(\beta, p), \quad (\text{E.12})$$

with  $x = e^{\beta(1 - \cos \frac{2\pi}{p})}/3$ .

In performing the summation in Eq. (E.12), we assumed a sufficiently low temperature so that  $x > 1$ , and  $\bar{w}$  is a monotonically decreasing function of  $\beta$ . Notably,  $\bar{w}$  can be made arbitrarily close to zero for large enough  $\beta$ . Let us denote by  $\beta_{\text{Peierls}}$  the solution to the equation  $\bar{w}(\beta_{\text{Peierls}}, p) = \frac{p-1}{p}$ . Then, for  $\beta > \beta_{\text{Peierls}}$ , the probability of the spin at the origin being the same as that on the boundary is  $\mathcal{P}(\theta_0 = \theta_{\infty}) > 1/p$ . In other words, for  $T < T_{\text{Peierls}}$ , we clearly have SSB. It is important to emphasize that  $T_{\text{Peierls}}$  is only a lower bound to the transition temperature, and the actual SSB occurs for  $T^{(1)} > T_{\text{Peierls}}$ . An estimate for  $T_{\text{Peierls}}$  resulting from this analysis

is  $T_{\text{Peierls}} \approx (1 - \cos \frac{2\pi}{p}) / \ln 6$  ( $\sim \mathcal{O}(1/p^2)$  for large  $p$ ). As in the lower bound derived herein, the energy cost for a domain wall is anticipated to determine the actual ordering temperature. This bound is *rigorous*. Physically, in Eq. (E.10), the logarithms of the two terms  $N_\ell$  and  $D_\ell$  capture, respectively, bounds on the entropy and energy costs associated with domain walls of length  $\ell$ .

Discrete vortices such as the one shown in Fig. 5 with a typical change of angle  $\Delta\theta = \mathcal{O}(1)$  (or  $|\Delta s| = \mathcal{O}(p)$ ) across the intersecting domain walls that extend over a linear distance  $\ell$  may entail, for all  $p \geq 5$ , an energy cost that scales as  $\ell$ . This is to be contrasted with the minimal energy penalty associated with a difference in angle of  $|\Delta\theta| = 2\pi/p$  for which the corresponding energy penalty as  $\ell/p^2$  (and that physically sets the bounds that we derived in the Peierls argument above). Thus, from energy-versus-entropy balance considerations, the temperature below which it is unfavorable to have vortices is  $T_{\text{Vortex}} \sim \mathcal{O}(1)$  (or of order  $J$ ): the energy for such domain walls scales as  $\ell$  as does the entropy associated with a network of possible intersecting domain walls that have a total length  $\ell$ .

## Appendix F. Proof of monotonicity of the correlation function $G$

We now prove Eq. (110) for large (yet finite) lattices. In finite size systems (no matter how large), there are no thermodynamic phase transitions. Thus, the free energy and all its derivatives (including, in particular, the two-point correlation function  $G(|\mathbf{r} - \mathbf{r}'|, T)$ ) are analytic for all values of  $\beta$ . We will prove monotonicity by expanding (the analytic)  $G$  as a power series in  $\beta$ , which is everywhere convergent, and illustrate that the coefficients multiplying each power of  $\beta$  are non-negative. The uniformity of the sign of all contributions to the series coefficients follows from repeated applications of the identity

$$S_p(n) = \sum_{s=0}^{p-1} e^{i\frac{2\pi n}{p}s} = p \delta_{n,0}, \quad (\text{F.1})$$

with the Kronecker delta above defined mod( $p$ ). That is,  $\delta_{0,0} = \delta_{\pm p,0} = \delta_{\pm 2p,0} = \dots = 1$ , otherwise it vanishes.

Longhand, the correlator  $G(|\mathbf{r} - \mathbf{r}'|, T)$  is given by ( $K = \beta J \geq 0$ )

$$\langle \cos(\theta_{\mathbf{r}} - \theta_{\mathbf{r}'}) \rangle = \frac{\sum_{\{\theta_{\mathbf{x}}\}} \cos(\theta_{\mathbf{r}} - \theta_{\mathbf{r}'}) \exp \left[ \sum_{\mathbf{x}} \sum_{\mu=1,2} K \cos(\theta_{\mathbf{x}+e_{\mu}} - \theta_{\mathbf{x}}) \right]}{\mathcal{Z}_p[K]}, \quad (\text{F.2})$$

with  $\theta_{\mathbf{r}} = 2\pi s_{\mathbf{r}}/p$ .

We Taylor expand the argument of the exponential, i.e.,  $\exp[\beta A] = \mathbf{1} + \beta A + (\beta A)^2/2! + \dots$ , in both the numerator and the denominator of Eq. (F.2), and may represent pictorially the expansion terms by Feynman-type diagrams. In this scheme, each appearance of  $\cos(\theta_{\mathbf{x}'} - \theta_{\mathbf{x}})$  relates to an internal propagator linking sites  $\mathbf{x}$  and  $\mathbf{x}'$ . Similar to perturbative schemes in the continuum, where the number of Feynman-type ‘‘bubble diagrams’’ in  $\mathcal{Z}_p[K]$  with nearest-neighbor links that share common vertices with any given ‘‘connected’’ diagram which contains both the sites  $\mathbf{r}$  and  $\mathbf{r}'$  is negligible, there is a near cancellation, in Eq. (F.2), of all ‘‘bubble diagrams’’. What remains from the ratio of Eq. (F.2) is the sum of all diagrams in which sites  $\mathbf{r}$  and  $\mathbf{r}'$  are linked to each other by the line stemming from  $\cos(\theta_{\mathbf{r}} - \theta_{\mathbf{r}'})$  as well as internal lines which pass through the points  $\mathbf{x} = 1, 2, \dots, m$ . Up to (inherently positive) symmetry factors, the numerical value of any such resulting diagram is given by a sum of the form

$$\sum_{s_{\mathbf{r}}, s_1, s_2, \dots, s_m, s_{\mathbf{r}'}=0}^{p-1} \beta^{t_{\mathbf{r}1} + t_{\mathbf{r}2} + \dots + t_{12} + \dots + t_{m\mathbf{r}'}} \cos(\theta_{\mathbf{r}} - \theta_{\mathbf{r}'}) (\cos(\theta_{\mathbf{r}} - \theta_1))^{t_{\mathbf{r}1}} \\ \times (\cos(\theta_{\mathbf{r}} - \theta_2))^{t_{\mathbf{r}2}} \dots (\cos(\theta_1 - \theta_2))^{t_{12}} \dots (\cos(\theta_m - \theta_{\mathbf{r}'}))^{t_{m\mathbf{r}'}} , \quad (\text{F.3})$$

where the integers  $t_{ab} > 0$  represent the number of lines linking sites  $a$  and  $b$ . It is simple to show that sums of the form of Eq. (F.3) are manifestly non-negative. Replacing  $\cos(\theta_a - \theta_b)$  by  $(\exp(i(\theta_a - \theta_b)) + \exp(i(\theta_b - \theta_a)))/2$ , a sum of exponentials with positive weights, Eq. (F.3) reduces to a sum of individual products with positive weights, each being of the form

$$\prod_{\mathbf{x}=\mathbf{r}, 1, 2, \dots, m, \mathbf{r}'} S_p(n_{\mathbf{x}}) \geq 0, \quad (\text{F.4})$$

with  $n_a$  set by sums of the powers  $t_{ab}$  in Eq. (F.3). Then, it follows that when the ratio of Eq. (F.2) is expanded in  $\beta$ , i.e.,  $G(|\mathbf{r} - \mathbf{r}'|, T) = \sum_t a_t \beta^t$ , the prefactor  $a_t$  multiplying each individual power  $\beta^t$  is non-negative. As such,  $G(|\mathbf{r} - \mathbf{r}'|, T)$  is manifestly monotonic in  $\beta$ , i.e.,  $\partial_{\beta} G(|\mathbf{r} - \mathbf{r}'|, T) \geq 0$ .

## References

- [1] R. Potts, Proc. Camb. Philos. Soc. **48**, 106 (1952).
- [2] F. Y. Wu, Rev. Mod. Phys. **54**, 235 (1982).
- [3] V. L. Berezinskii, Sov. Phys. JETP **32**, 493 (1971).
- [4] J. Kosterlitz and D. Thouless, J. Phys. C **6**, 1181 (1973).
- [5] J. Kosterlitz, J. Phys. C **7**, 1046 (1974).
- [6] J. V. José, L. P. Kadanoff, S. Kirkpatrick, and D. R. Nelson, Phys. Rev. B **16**, 1217 (1977).
- [7] P. Minnhagen, Rev. Mod. Phys. **59**, 1001 (1987).
- [8] D. B. Abraham, *Surface Structures and Phase Transitions - Exact Results*, in *Phase Transitions and Critical Phenomena* Vol. 10, edited by C. Domb and J. L. Lebowitz (Academic Press, 1986) p. 1.
- [9] D. R. Nelson and Halperin, Phys. Rev. B **19**, 2457 (1979); A. P. Young, Phys. Rev. B **19**, 1855 (1979).
- [10] S. Elitzur, R. B. Pearson, and J. Shigemitsu, Phys. Rev. D **19**, 3698 (1979).
- [11] H. Nishimori and G. Ortiz, *Elements of Phase Transitions and Critical Phenomena* (Oxford University Press, 2011).
- [12] E. Cobanera, G. Ortiz, and Z. Nussinov, Phys. Rev. Lett. **104**, 020402 (2010).
- [13] E. Cobanera, G. Ortiz, and Z. Nussinov, arXiv:1103.2776v1 [cond-mat.stat-mech].
- [14] Z. Nussinov and G. Ortiz, Phys. Rev. B **79**, 214440 (2009).
- [15] Z. Nussinov and G. Ortiz, Europhysics Lett. **84**, 36005 (2008).
- [16] J. Villain, J. Phys. (Paris) **36**, 581 (1975).
- [17] R. Savit, Rev. Mod. Phys. **52**, 453 (1980).

- [18] M. B. Einhorn, R. Savit, and E. Rabinovici, *Nuc. Phys. B* **170**, 16 (1980).
- [19] C. M. Lapilli, P. Pfeifer, and C. Wexler, *Phys. Rev. Lett.* **96**, 140603 (2006).
- [20] J. L. Cardy, *J. Phys. A: Math. Gen.* **13**, 1507 (1980).
- [21] J. Fröhlich and T. Spencer, *Comm. Math. Phys.* **81**, 527 (1981).
- [22] O. Borisenko, G. Cortese, R. Fiore, M. Gravina, and A. Papa, *Phys. Rev. E* **83**, 041120 (2011). This work presents a summary of current debates in its introduction.
- [23] Y. Tomita and Y. Okabe, *Phys. Rev. B* **65**, 184405 (2002).
- [24] V. A. Malyshev and E. N. Petrova, *J. Math. Sciences* **21**, 877 (1983).
- [25] J. Schwinger, *Quantum Mechanics: Symbolism of Atomic Measurements* (Springer Verlag, Berlin, 2001).
- [26] P. J. Davis, *Circulant Matrices* (John Wiley, New York, 1979).
- [27] M. Henkel, *Conformal invariance and critical phenomena* (Springer Verlag, Berlin, 1999).
- [28] *Handbook of Mathematical Functions*, edited by M. Abramowitz and I. A. Stegun (Dover, New York, 1972).
- [29] V. B. Matveev, *Inverse Probl.* **17**, 633 (2001).
- [30] J. J. Rotman, *An Introduction to the Theory of Groups* (Springer Verlag, New York, 1999). See specially Chapter 11, Example 11.5 on page 347.
- [31] C. D. Batista and G. Ortiz, *Adv. in Phys.* **53**, 2 (2004).
- [32] For  $p = 4$  we may represent the four equidistant spin orientations on the unit circle in terms of the normalized two component spin vectors  $(\chi_{\mathbf{r}}^1, \chi_{\mathbf{r}}^2)/\sqrt{2}$  at sites  $\mathbf{r}$  with  $\chi_{\mathbf{r}}^{1,2} = \pm 1$ . With this representation, the isotropic partition function reads

$$\mathcal{Z}_{p=4}[K] = \sum_{\{\chi_{\mathbf{r}}^1, \chi_{\mathbf{r}}^2\}} \exp \left[ \sum_{\mathbf{r}} \sum_{\mu=1,2} K(\chi_{\mathbf{r}}^1 \chi_{\mathbf{r}+\mathbf{e}_{\mu}}^1 + \chi_{\mathbf{r}}^2 \chi_{\mathbf{r}+\mathbf{e}_{\mu}}^2)/2 \right], \quad (\text{F.5})$$

which shows that the  $p = 4$  clock model is equivalent to two decoupled Ising systems.

[33] For  $p \geq 3$ , ground states that are also eigenstates of  $\mathcal{C}_0$ ,  $\mathcal{C}_0|\tilde{\Psi}_\pm^s\rangle = \pm|\tilde{\Psi}_\pm^s\rangle$ , can be constructed:

(i)  $p \in \text{odd}$ :

$$\begin{cases} |\tilde{\Psi}_+^0\rangle = |\Psi_0^0\rangle \\ |\tilde{\Psi}_\pm^s\rangle = (|\Psi_0^s\rangle \pm |\Psi_0^{p-s}\rangle)/\sqrt{2}, \text{ for } 1 \leq s \leq (p-1)/2, \end{cases}$$

(ii)  $p \in \text{even}$ :

$$\begin{cases} |\tilde{\Psi}_+^0\rangle = |\Psi_0^0\rangle, |\tilde{\Psi}_+^{p/2}\rangle = |\Psi_0^{p/2}\rangle \\ |\tilde{\Psi}_\pm^s\rangle = (|\Psi_0^s\rangle \pm |\Psi_0^{p-s}\rangle)/\sqrt{2}, \text{ for } 1 \leq s \leq p/2 - 1 \end{cases} .$$

[34] R. B. Griffiths, J. Math. Phys. **8**, 478 (1967).

[35] G. Rideau, Lett. Math. Phys. **24**, 147 (1992).

[36] K. Kowalski, J. Rembielinski, and L. C. Papaloucas, J. Phys. A: Math. Gen. **29**, 4149 (1996).